Pacific Northwest
NATIONAL LABORATORY

PNNL-33503

Lithium-Ion Battery Design for Grid-Scale Energy Storage App

September 2022

Liu, Dianying
Kondyukov, Grigoriy
Zhou, Huifeng

U.S. DEPARTMENT OF ENERGY

Prepared for the U.S. Department of Energy
under Contract DE-AC05-76RL01830

PACIFIC NORTHWEST NATIONAL LABORATORY
operated by
BATTELLE
for the
UNITED STATES DEPARTMENT OF ENERGY
under Contract DE-AC05-76RL01830

Printed in the United States of America

Available to DOE and DOE contractors from
the Office of Scientific and Technical Information,
P.O. Box 62, Oak Ridge, TN 37831-0062
www.osti.gov
ph: (865) 576-8401
fax: (865) 576-5728
email: reports@osti.gov

Available to the public from the National Technical Information Service
5301 Shawnee Rd., Alexandria, VA 22312
ph: (800) 553-NTIS (6847)
or (703) 605-6000
email: info@ntis.gov
Online ordering: http://www.ntis.gov

PNNL-33503

Lithium-Ion Battery Design for Grid-Scale Energy Storage App

September 2022

Liu, Dianying
Kondyukov, Grigoriy
Zhou, Huifeng

Prepared for
the U.S. Department of Energy
under Contract DE-AC05-76RL01830

Pacific Northwest National Laboratory
Richland, Washington 99354

Abstract

A software that delivers parameters from energy storage system (ESS) to container, rack, module and single cell design, as well as data analysis on arbitrage energy and frequency regulation of ESS in different regions, has been developed. The Lithium-ion Battery Design for Grid-scale Energy Storage App V1.0 has the capability to output the system, module and cell design with the energy, power, capacity, group method, cost of single cell, and single cell test protocol which break down from input energy storage system data in different regions. The default chemistry of the battery is $LiFePO_4$ and graphite. The energy density of the graphite/$LiFePO_4$ pouch cell ranges from 100 Wh/kg to 200 Wh/Kg in the software. Graphite/$LiFePO_4$ pouch cell (up to 1Ah in lab) manufacturing line is also built and can be used to evaluate the test protocol, moreover, for electrolyte evaluation in other ESMI seedling projects. The software enables rapid prototyping to accelerate energy storage research, development, and manufacturing.

Acknowledgments

This research was supported by the Energy Storage Materials Initiative (ESMI), under the Laboratory Directed Research and Development (LDRD) Program as a strategic investment at Pacific Northwest National Laboratory (PNNL). PNNL is a multiprogram national laboratory operated for the U.S. Department of Energy (DOE) by Battelle Memorial Institute under Contract No. DE-AC05-76RL01830.

Contents

1.0 Introduction

Large-scale electrical energy storage has received worldwide attention for reducing fossil energy consumption in automobiles (transportation application) and for the widespread use of intermittent renewable energy in the modern electrical grid (stationary application). However, most of today's batteries for grid storage were never specifically designed to meet the demands of the grid but were instead adapted from other applications in which volumetric/specific energy and power are the key requirements. For example, 90% of the market for today's stationary energy storage is served by li-ion batteries, however most of those batteries have been manufactured in the same designs as those used in electric vehicles (EVs) because the performance metrics required for both applications are compatible, but they are still far from meeting the grid's storage needs such as low cost, long cycle life, reliable safety and reasonable energy density. [1]

In addition, today's battery design for grid storage failed to cope with geographical diversity. The geographical regions of North America are diverse, and so too are the requirement for the battery design for grid storage. For instance, in the Pacific Northwest where there is significant hydropower capacity along with the Columbia and Snake River systems, rapid snowmelt could result in energy production by dams that exceed the region's demand for electricity. [2] Because of regional differences in the distribution of renewable resources and the structural differences in the transmission and generation mix, custom-designed cell for each region is required to better match the supply of renewable resources with demand via increased spatial diversity, time-shiftable load, or energy storage.

The significant improvement over the existing approach to grid-scale energy storage is that the proposed approach provides a fundamentally novel approach and integrated strategy to build a low-cost and highly safe battery composed of cost-effective active materials with chemically and structurally engineered interfaces and advanced cell geometries combined with a data-driven, machine-learning method for adaptive design approach to deal with geographically diversified cell performance specifications.

New types of energy storage with characteristics including reduced battery cost, extended cycle life, enhanced safety as well as reasonable energy density is critical for future scaled battery module/pack [3]. In this regard, batteries with electrode materials made from low-cost, earth-abundant elements are needed to meet the requirements of sustainable energy systems. Among the cathode materials, olivine lithium iron phosphate ($LiFePO_4$, LFP) has merits of cost-effectiveness due to much lower cost of iron precursor comparing with Ni or Co-containing layered oxides, e.g., $LiCoO_2$ (NCA), $LiNi_{1/3}Mn_{1/3}Co_{1/3}O_2$ (NMC111), and $LiNi_{0.80}Co_{0.15}Al_{0.05}O_2$ (NCA). Moreover, LFP cathode has unique merits for the grid-scale application due to high thermal stability for safety and low toxicity. For the anode couple, graphite is still effective due to its performance reliability in Li-ion chemistry and less contribution to battery cost. For instance, their material costs are \$5~10/kg and \$10~20/kg for natural and artificial graphite materials, respectively. Therefore, the graphite/LFP couple system is suitable for the grid-scale application. In practice, the graphite/LFP system is designed for high-power applications. For example, commercial cells produced by A123 Systems [4] consist of carbon-coated LFP (C–LFP) cathode and graphite anode.

Recently, PNNL has released an analogous software for Li-metal pouch cell design (see Fig. 1) supported by the Battery 500 Consortium.[5] In this work, we will leverage our battery design software experience and grid energy storage data from different regions to develop software specifically for energy storage batteries based on chemistries and battery design from lithium metal batteries as well as lithium-ion batteries.

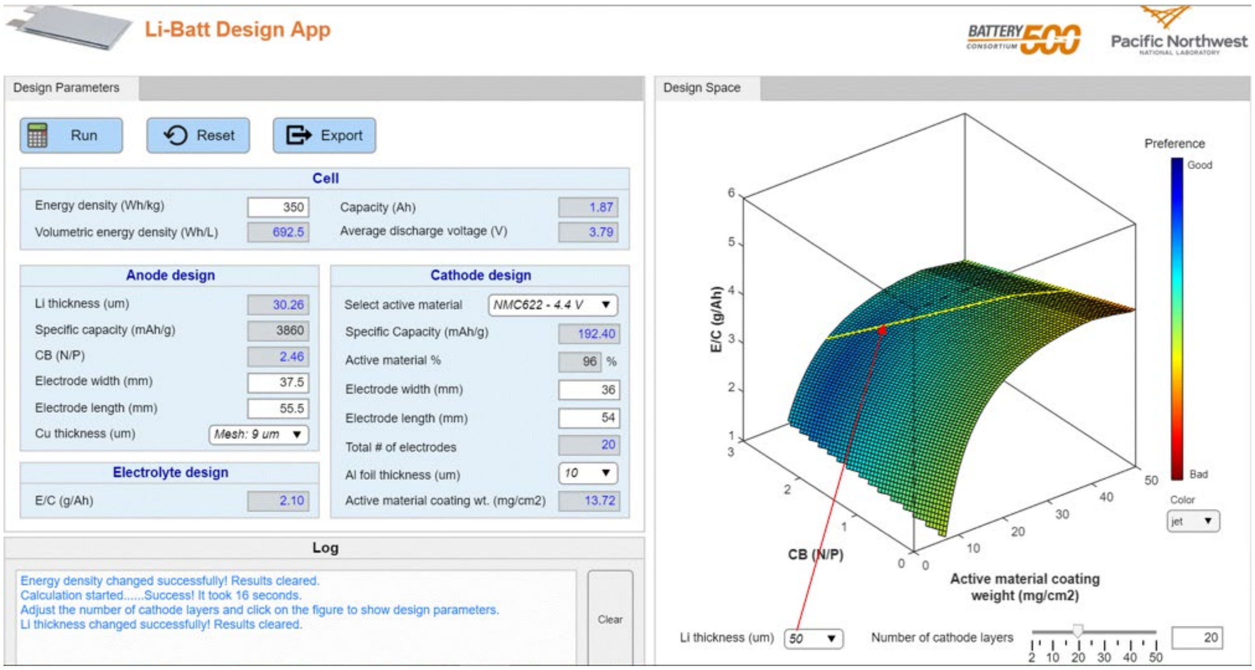

Figure 1. Software for Li metal pouch cell design by batt500.

2.0 Method, Discussion, and Results

The software development work is divided into two parts: 1) ESS system break down and cell design; 2) ESS data analysis, like arbitrage energy and frequency regulation. The software will help the user to break down the ESS system with required energy and power, and then build user's own battery. Figure 2 shows the workflow of the cell design in software for energy storage Li-ion battery. First, the user inputs the requirements of the ESS battery in the software, then the software automatically analyzes the inputted parameters, the software performs the cell design according to the inputted requirements and finally exports the detailed designs information and estimated performances.

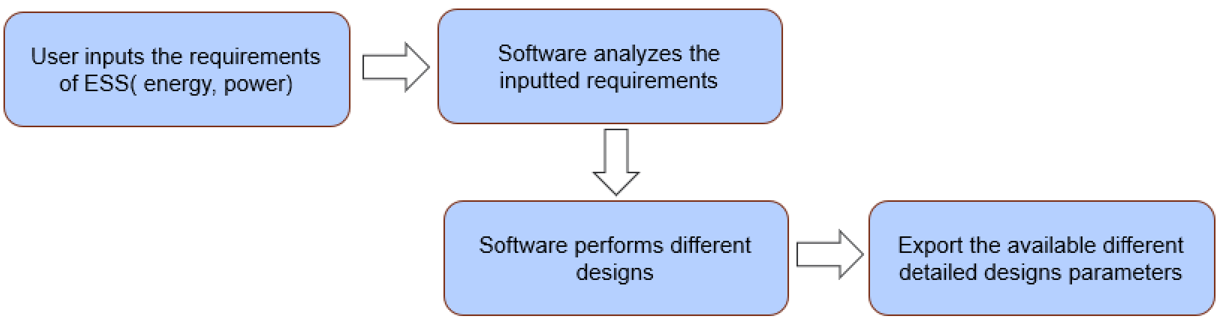

Figure 2. Workflow chart of battery design in software.

2.1 Energy storage system breakdown and battery design software

As show in Figure 3, the ESS system is comprised of container, rack, module, and single cell. A grid-level ESS system will have many containers connected in parallel and in serial (Figure 4) to reach the target energy and power. Each container contains several racks connected in parallel and in serial (Figure 5). Each rack contains several modules connected in parallel and in serial (Figure 6). Note that, sometimes, pack is used and has several modules in it, like in an electrical vehicle. Here, most of the battery vendor prefers to provide a large module instead of a pack in ESS application, reducing the complexity and cost of the system. Module will be adopted to be the unit broken down from rack. Each module has several single cells, or several ten single cells connected in parallel and in serial (Figure 7).

To determinate the energy and voltage of a component, it's critical to figure out how many sub-units used and connected in what way. Theoretically, in pure mathematic, one can have thousands of combinations of sub-units to achieve a component with required energy and voltage. However, consider the practical conditions, such as space, the complexity of the manufacturing and working voltage of the component, the vendors prefer to certain group method, like two units connected in parallel, 2PxxxS. The power of the system depends on the cell design, like the material and its particle size distribution, coating weight, pressing density, tortuosity. The rate of the cell can be related to the power/energy ratio of the ESS. For example, an ESS system has 100 MWh of energy and requires the output power of 20 MW. The power/energy ratio is 0.2. So, the c-rate of the single cell is closed to 0.2C, considering the voltage polarization is small, ca.90-95% for graphite/LFP single cell. This way, we will focus on the energy and voltage for the ESS breakdown.

To make the group method easily and completely, in this work, we define SN: number of unites connected in serial; PN: number of containers connected in parallel; KN: number of knot. Note that, knot is not an industry term, knot is used here to describe the repeat unit of a group including SN and PN. With this definition, all the group methods of units in a component are involved. The unit can be container (Figure 4), rack (Figure 5), module (Figure 6) and single cell (Figure 7). For example, there are several single cells connected with SN=5, PN=2, KN=1 in a module, that translates to a string of 5 single cells connected in serial and parallelized with another string of 5 single cells connected in serial. Note that PN≠1, it starts from 0, 2, 3, 4, …as it makes no sense a string of batteries is parallelized to itself, we define PN=0 if no parallel battery exists. The software will output all the combinations of SN, PN and KN relating to the input energy of the ESS. User can choose the interested combination/group method to break down the ESS system to a single cell based on the real application, constrained by working voltage, space, manufacturing complexity .etc.

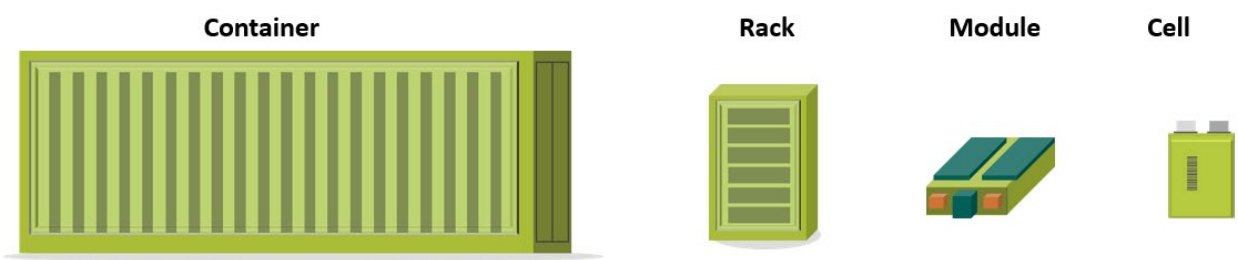

Figure 3. ESS components: from container to cell.

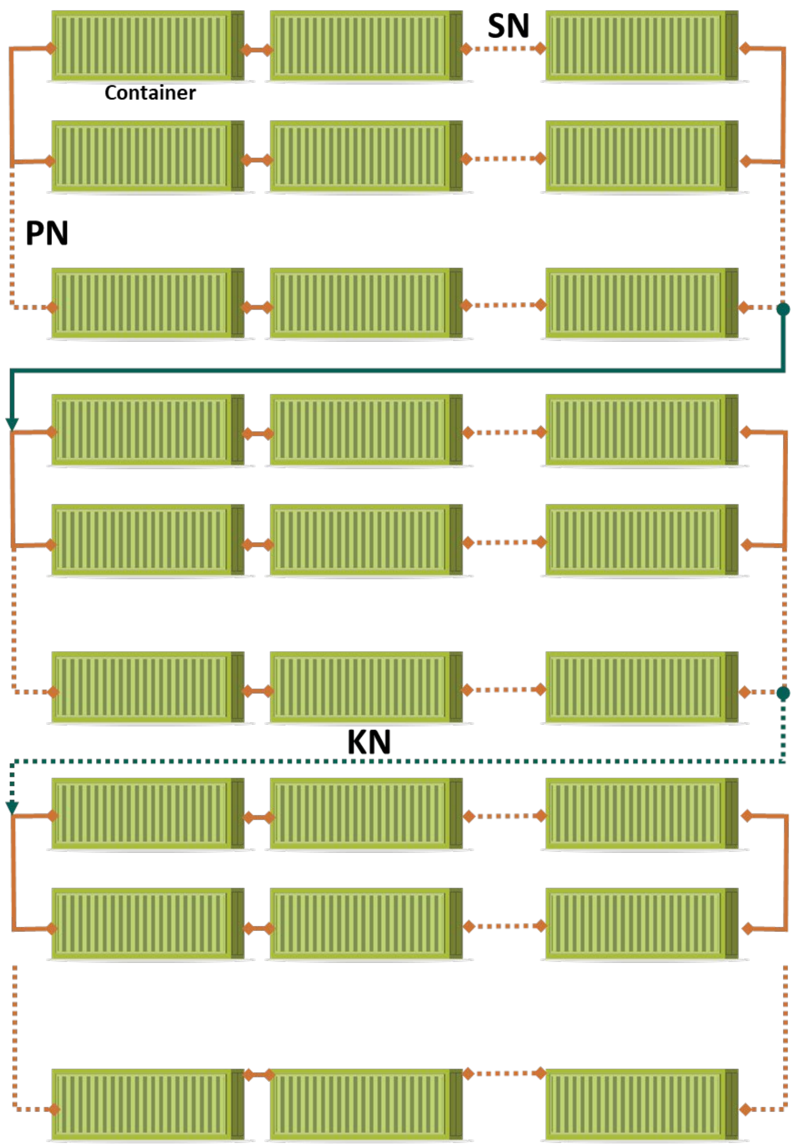

Figure 4. Containers and their connections in an ESS.

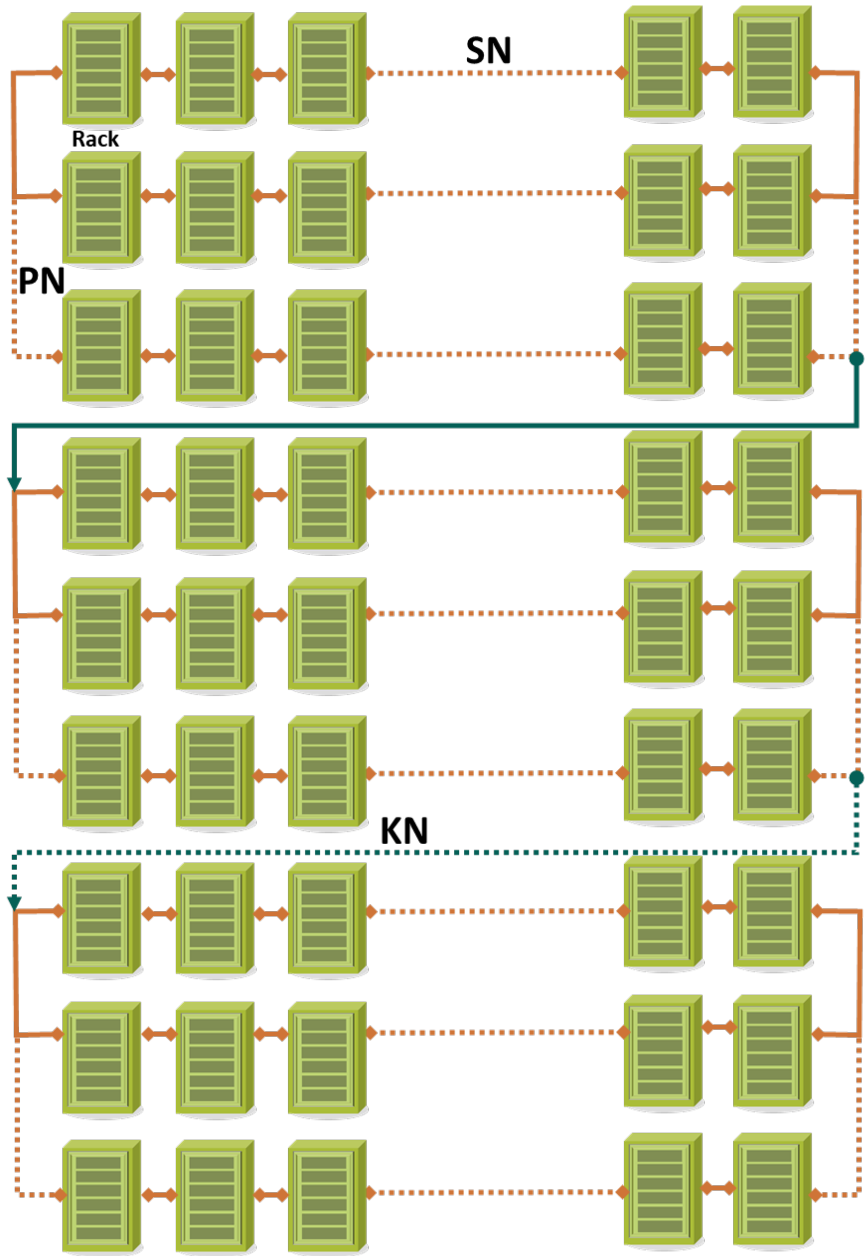

Figure 5. Racks and their connections in a container.

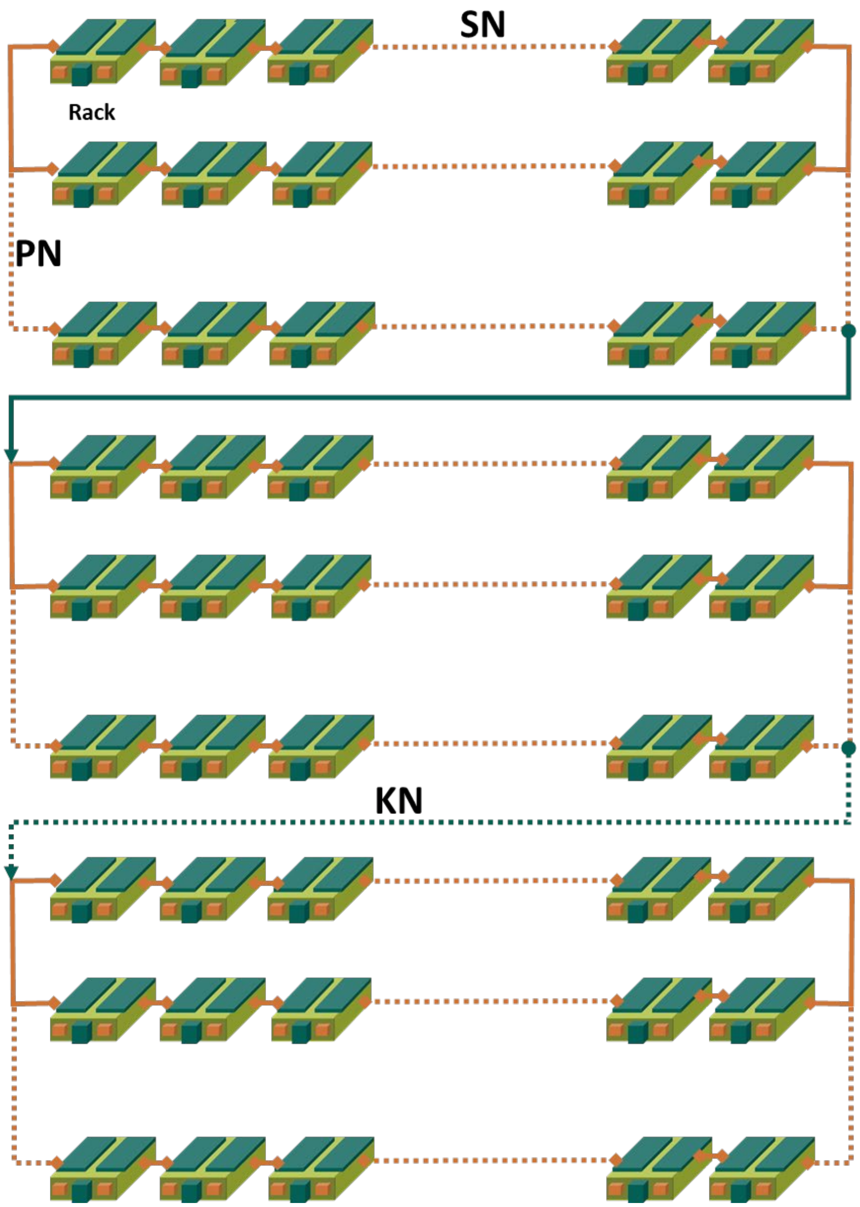

Figure 6. Modules and their connections in a rack.

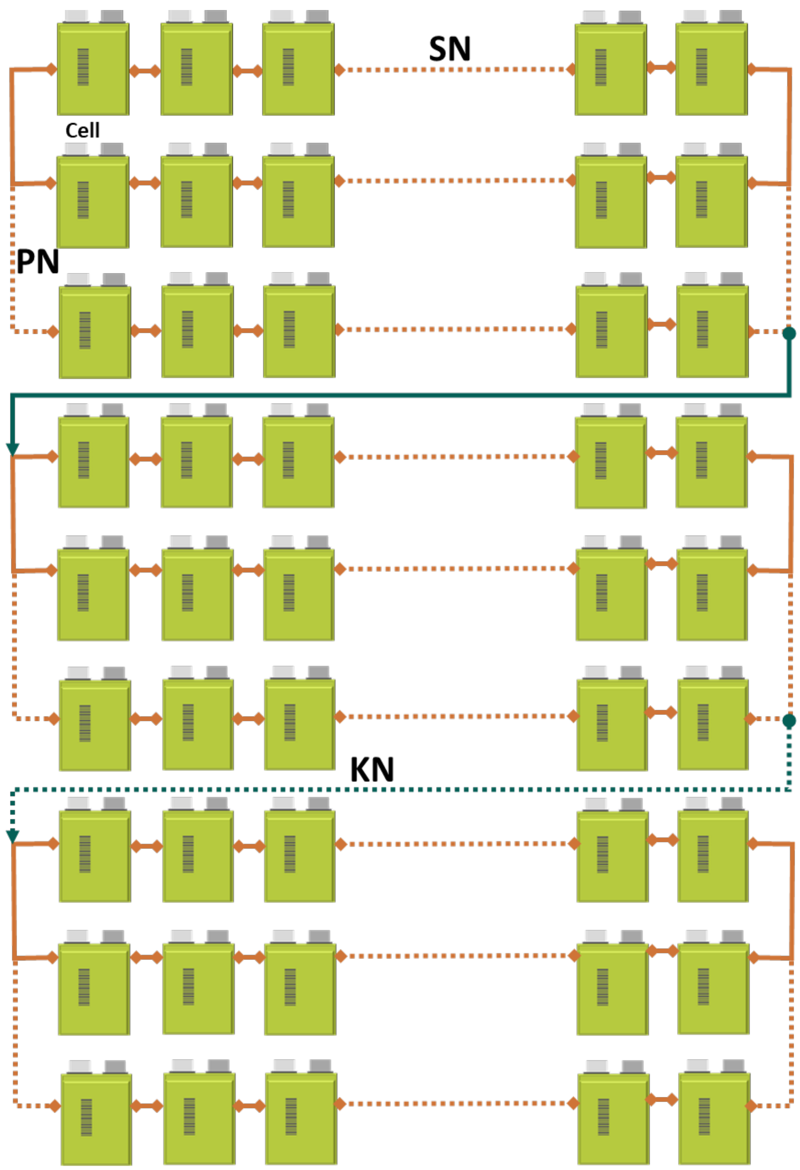

Figure 7. Single cells and their connections in a module.

After confirming the group methods of a component, it's easy to figure out the energy of the component so that the ESS breakdown work can be proceeded successfully. As showed in Figure 7a, in a 20MW/100MWh ESS system, after the user input 20MW and 100 MWh in the software, the user will be directed to step 2-container, here it will show a 3D ternary plot containing the energy of the container with all group methods. If user click the data point in the plot and figure out the interested group method (PN, SN, KN=2, 4, 3), he/she will be directed to step 3-rack. At same time, the software will fill the working voltage of the container with selected group methods. The rack and module breakdown are same as container breakdown. Finally, all the energy of the components, working voltage and group methods will be provided by the software.

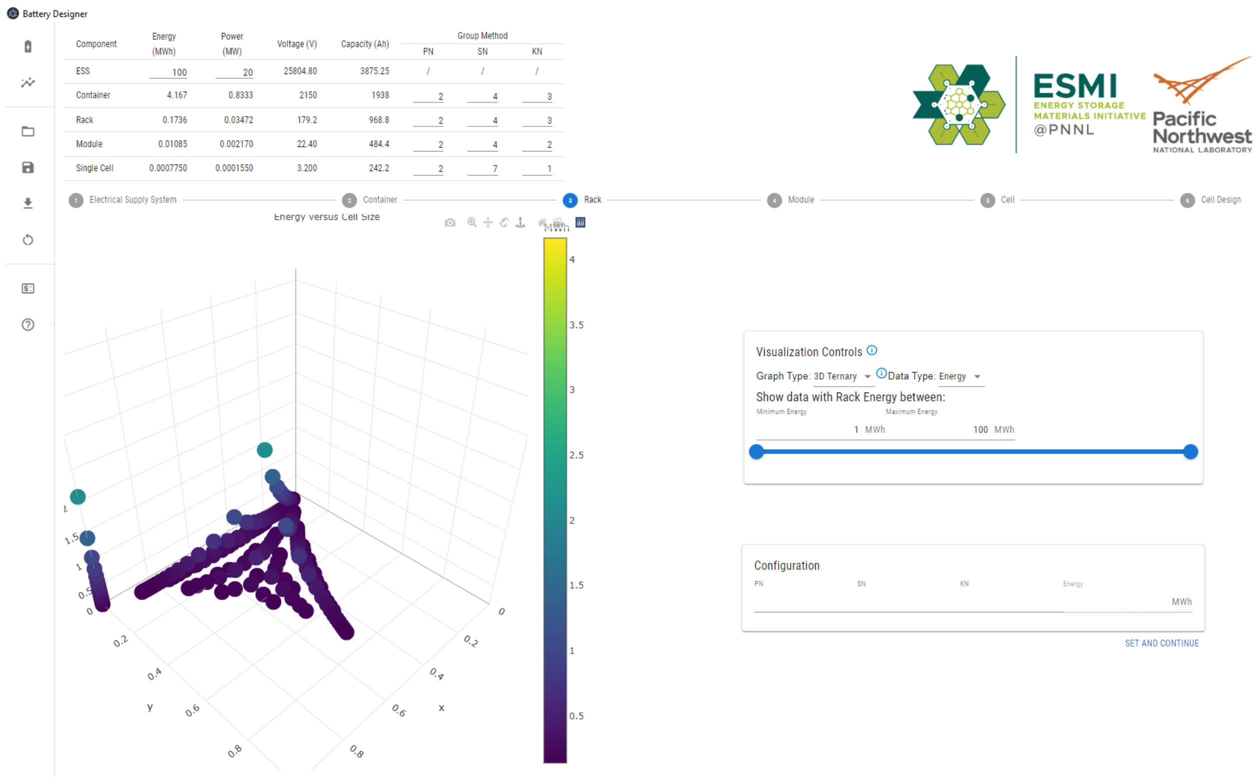

Figure 7a. Breakdown of 20MW/100MWh ESS system.

When the ESS broke down to a single cell with above method, the capacity of the single cell will be provided by the software. The voltage of graphite/LFP pouch cell is fixed to 3.2V. The pouch cell battery with the LFP/Gr. chemistry has been studied and produced extensively in industry. As shown in Figure.8, the jellyroll is produced by a stacking process with alternative cathode sheet, separator sheet and anode sheet. Here, we focus on the graphite/LFP pouch cell battery as this chemistry has long cycling life, low cost and high safety. The LFP active material will be mixed with binder and carbon additive with Al foil to produce the cathodes. The graphite material will be mixed with binder and carbon conductivity with Cu foil to produce the anodes. The software development is also based on this chemistry.

The cell design process in the software after having the capacity from ESS breakdown includes:

1. Calculate the capacity of different size. The size includes the thickness, length and width of the pouch cell. The thickness of the battery can be adjusting by the numbers of LFP cathode electrodes, from 1 to several hundreds. The length and width of the pouch cell is calculated by 1) length/width ratio, from 1 to 2, 0.05 for each step. These ratios include most of the battery size ratio in the market, like 1.1 to 1.3. 2) In each length/width ratio, another function with capacity calculation can be applied to calculate the length and width, capacity provided by ESS breakdown=Number of the LFP cathodes*coating weight*specific capacity*length*width. The coating weight and specific capacity will be provided by software according to the power/energy ratio. Therefore, at certain cathode layers and length/width ratio, the length and width of the pouch cell can be easily calculated.

2. Plot the energy density of the pouch cell relating to the size calculation. User just needs to set the data range, like size constrain, to view the provided cell design. The software will automatically provide the cell design having highest energy density.

3. Plot the weight distribution/cost distribution of the selected cell design. The cost estimation is just for the materials cost or bill of materials with the selected cell design, not include the manufacturing cost. The software will provide the default cost of each material/component at the time of software developed which is July 2022. The user can set the prices of each unit if known.

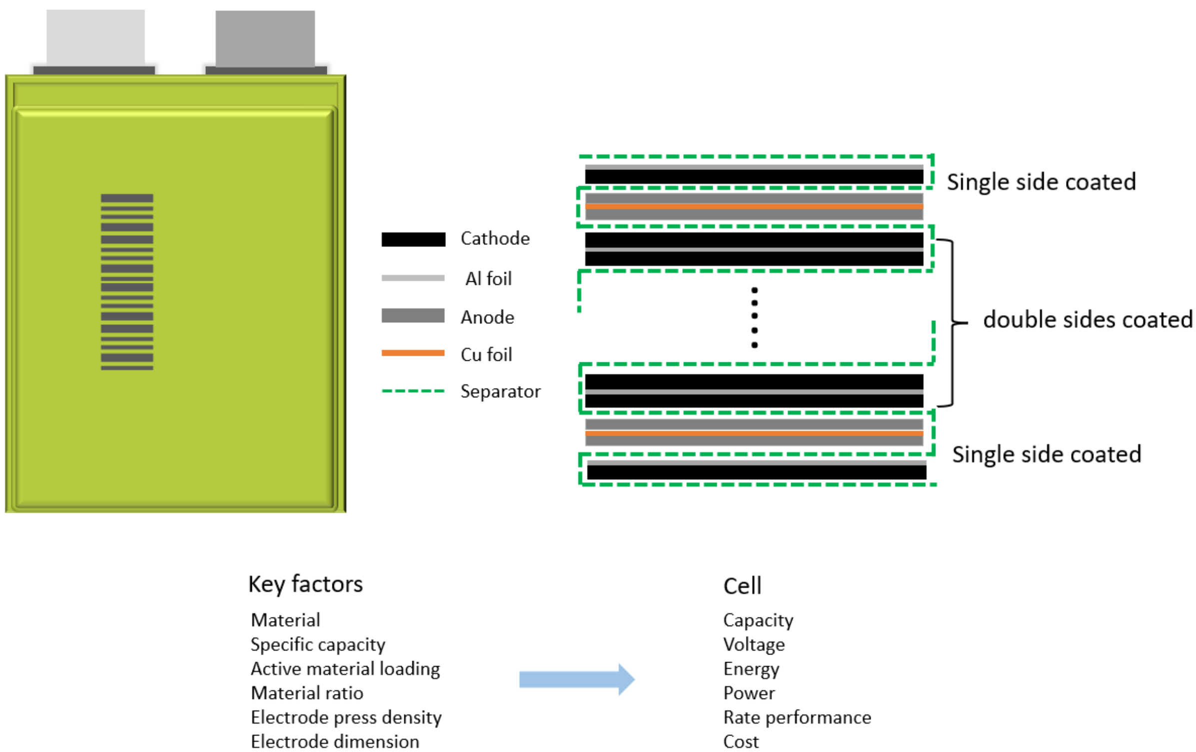

Figure 8. Schematic of Li-ion pouch cell battery and its relevant key factors and cell performances.

2.1.1. Data collection with LFP half-cell for design

The areal loading, percentage, ratio, pressing density of LFP cathodes, and its size will affect the energy and power of the graphite/LFP. Figuring out the relationships between these key factors and cell performances is crucial to develop the software. Figure 9 shows the one of design of experiments to collect and analysis data, then build the software. To simplify the design and most of the power/energy ratio in ESS is less than 1, we fixed the LFP percentage to 92% and investigate the reversible capacity changes along with the coating weight and rate. Here, 8 different LFP electrodes with coating weight from thin electrode to thick electrode, 1-3.5

mAh/cm^2, were produced. These LFP electrodes were coupled with Li metal to assemble the 2032 coin cell. The flooded electrolyte containing 1M $LiPF_6$ EC/EMC/DEC (1/1/1, by volume) + 1 wt.% VC+5wt.% FEC was applied. Two coin cells were assembled for each coating weight. These cells were tested between 2.2V and 3.5V with 1/10C, 1/8C, 1/5C, 1/4C, 1/3C, 1/2C , 1C and 2C. The testing results can be found in Figure 10 and Table 1. These results will provide the basic data supporting the calculation of the capacity of the single cell provided by the ESS breakdown work.

Note that, graphite electrodes with different coating weight were also tested from 1/10C to 2C. However, even for slightly thin electrodes, the specific capacity can't reach normal capacity as the commercial battery. So, here we just control the LFP electrode when performing the cell design, the graphite electrode will be designed with vendor's material data. The N/P ratio will be fixed to 1.2, slightly high as 1.1 in battery for consumer electronics as the cycling life in ESS requires to be 10-20 years.

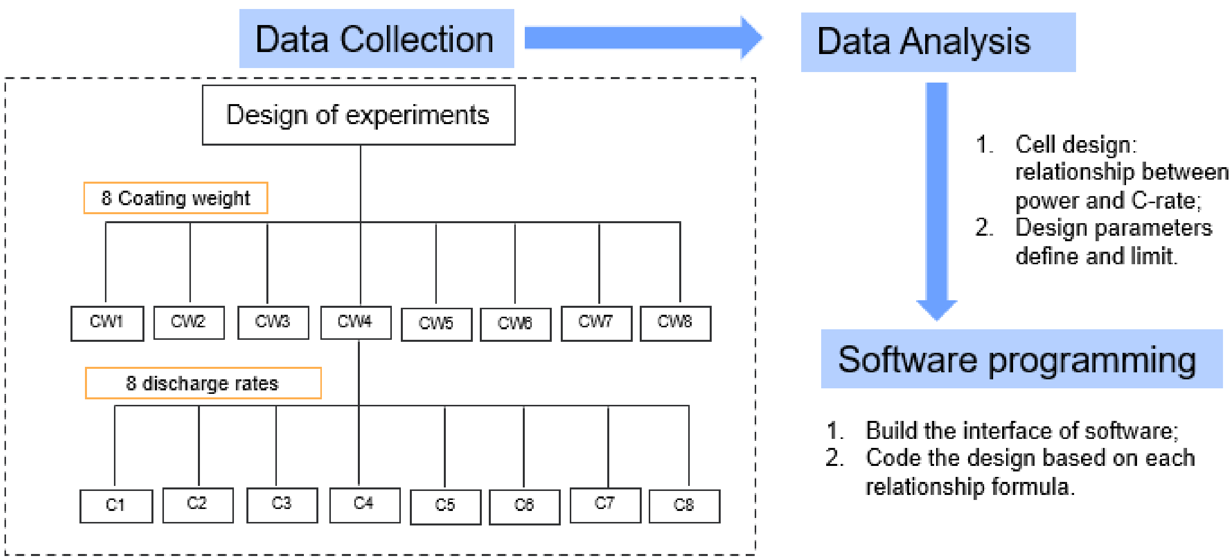

Figure 9. Method to build the software for graphite/LFP pouch cell design

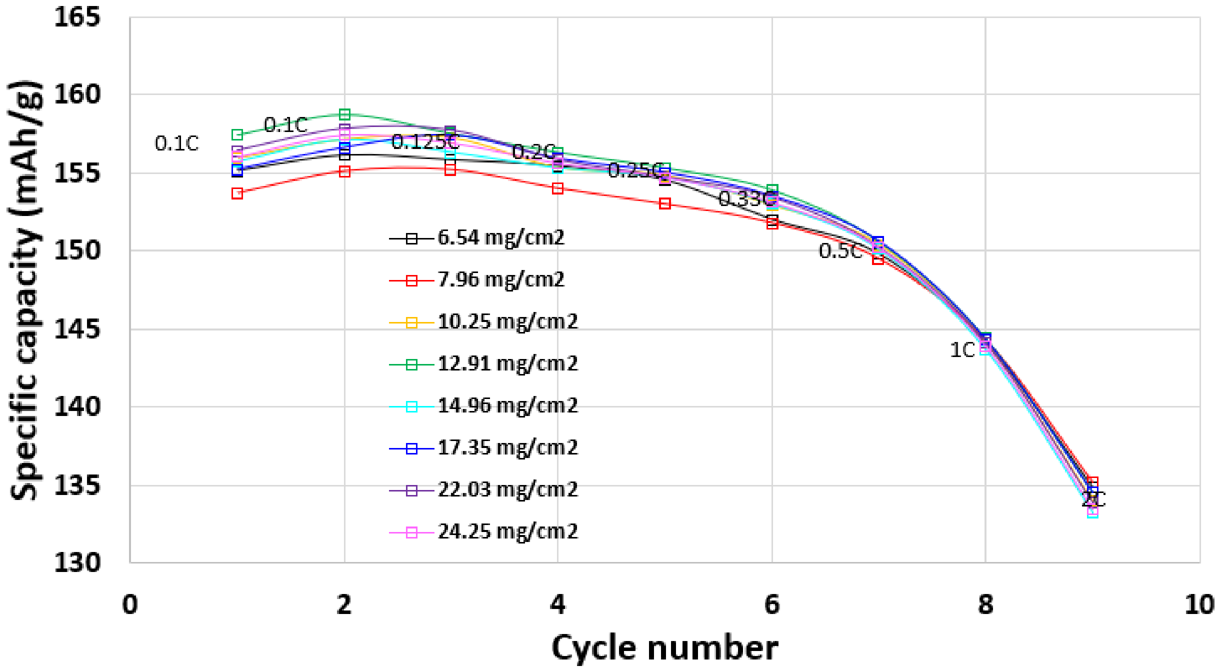

Figure 10. Rate performance of LFP cells with different loading

Table 1. Rate performance of LFP cells with different coating weight, 2.2-3.8V

Coating weight (mg/cm2)	Area capacity (mAh/cm2, 0.1C)	0.1C	0.125C	0.2C	0.25C	0.33C	0.5C	1C	2C
6.54	0.94	156.1	155.8	155.4	154.5	152	149.8	144.1	134.9
7.96	1.14	155.1	155.2	154	153	151.8	149.5	144.3	135.2
10.25	1.48	157.1	157.2	155.3	154.8	152.9	150.4	144.1	134
12.91	1.89	158.7	157.5	156.3	155.3	153.9	150.6	144.4	134.6
14.96	2.16	157.1	156.3	155.3	154.7	153	150.1	143.7	133.3
17.35	2.48	156.6	157.4	155.9	155	153.5	150.6	144.3	134.5
22.03	3.17	157.8	157.7	155.8	154.7	153.4	150.2	144.1	133.9
24.25	3.51	157.4	156.9	155.6	154.7	153.1	150.2	143.9	133.5

2.1.2. Tech stacks choose for software

We have looked over the available contemporary frameworks to build the closed-source desktop Battery Designer application. We evaluated them primarily on the permissibility of their licenses and potential iteration speed given the expiration. Electron mostly won out because of familiarity with React and uncertainty with how temperamental/difficult modification to design elements in other frameworks would be; HTML+CSS is straightforward. Its only real issue is needing 100Mb of RAM due to the bundled Chromium which runs the application but is otherwise very performant.

Proposed Tech stack:

Desktop Framework: Electron

Software Framework: React

Language: TypeScript/JavaScript + compiled dynamic binaries

Pros:

- MIT License (free + commercialization)
- Lots of open-source JavaScript libraries that can be used, specifically for graphing
- Can be ported as a web app with minimal changes
- React generates well-used HTML and CSS directly, unlike other widget-oriented frameworks.

Cons:

- Electron has a large memory footprint due to running its own Chromium instance. 100mb RAM usage at minimum.

Tech stacks considered with a brief comparison of their strengths and weaknesses:

Qt + Python:

Pros:

- Very good GUI tools
- Python libraries
- Efficient executable and system interfaces

Cons:

- Complex Licensing
    - GNU General Public license available free if source is distributed with software binary
    - Commercial license (~$500) required for closed-source binaries.

Kivy + Python:

Pros:

- MIT License
- Access to Open-Source Python Libraries
- Lightweight for resource usage

Cons:

- Underdeveloped GUI API + Community support

Go + Fyne:

Pros:

- MIT License
- Micro-executable
- Large community library

Cons:

- Go learning curve, libraries not as old or well-maintained as Python counterparts
- GUI API is underdeveloped

Flutter + Dart:

Pros:

- BSD License
- Lighter weight than Electron
- Great community support

Cons:

- Dart learning curve
- Many libraries are not open source (require commercial licensing)

C# + Windows Presentation Foundation:

Pros:

- Easy native windows development

Cons:

- No cross-platform compatibility

2.1.3. Software development

Final software

With the above design information/discussion on key parameters and cell performance, the final software is achieved. Fig.11 shows the interface of the design software.

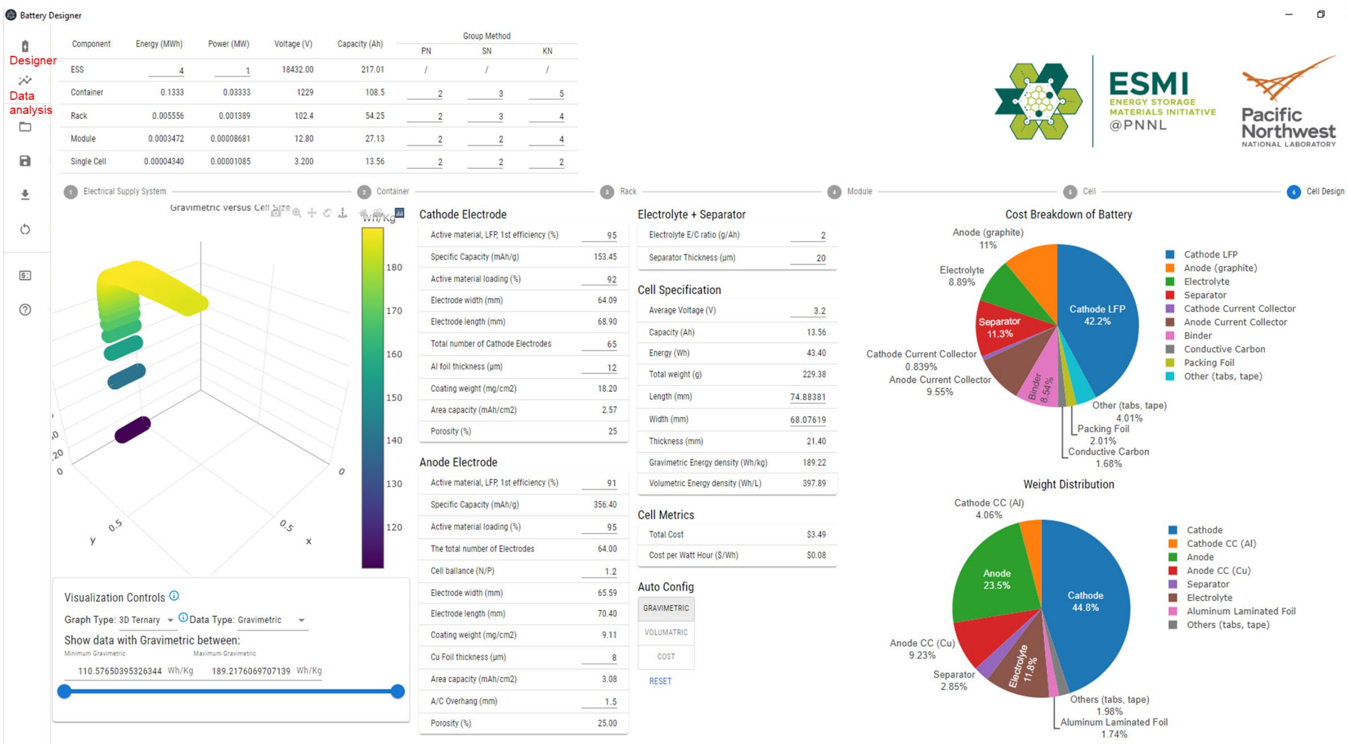

Figure 11. The interface of the Li-ion battery for grid-scale energy storage design app: Designer interface.

2.2 Energy storage data analysis and software development

Energy storage can provide various services (e.g., load shifting, energy management, frequency regulation, and grid stabilization) [6] to the power grid and its economic viability is receiving increasing attention. One of the most discussed revenue sources for energy storage is real-time temporal arbitrage and frequency regulation (i.e., charging at low prices and discharging at higher prices), where storage units take advantage of the price spreads in real-time electricity market prices to make profits over time [7].

2.2.1. Arbitrage energy data analysis

Energy arbitrage is a technique where power is bought during off-peak hours (when grid prices are cheapest). It is then stored and used during peak hours (when grid electricity prices are highest). Peak hours are typically from 10am-2pm and 6pm-10pm. Battery storage allows you to charge your battery outside of peak hours, when electricity is cheapest. Energy arbitrage means storing this energy for use during peak hours guarantees cheap electricity prices throughout the day.

For arbitrage energy analysis work, we choose MISO (Midcontinent Independent System Operator) with 1MW and 4 MWh arbitrage energy data in 2018 to get the single cycles.

The resolution of the arbitrage data is 1 hour. Figure 12 is the time series data of the arbitrage data, when the battery is taking the rest, the power is 0 and for a whole cycle the SOC is from 100 to 0 and 0 to 100. To study the data well, we split the time series data into individual cycles.

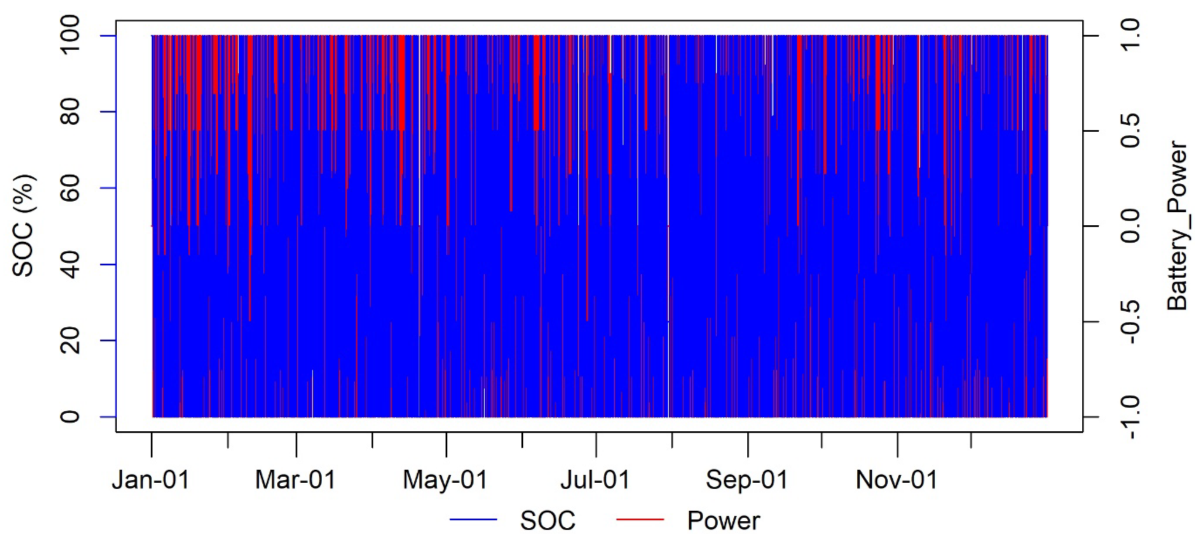

Figure 12. Time series plot of arbitrage data of 2018

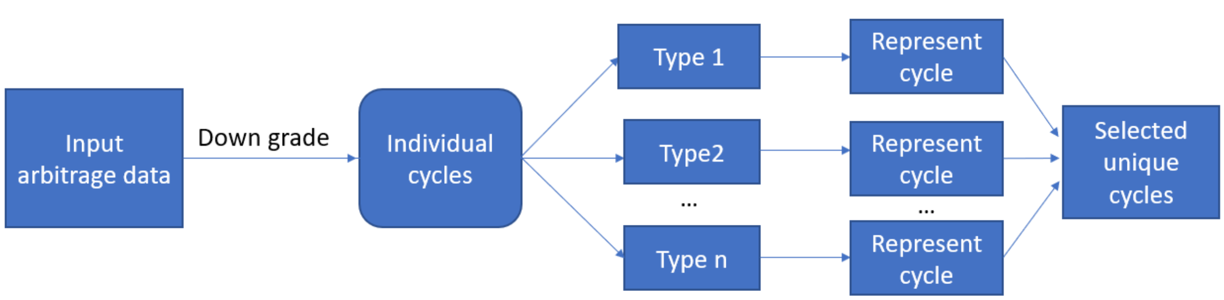

Figure 13. Workflow to get the selected unique cycles

The data was spilt into 412 individual cycles and some of the cycles have the similar patterns. To simplify those cycles, we grouped the 412 cycles into 36 groups. Table 1 shows the top 10 types which contain most cycles. The type of the unique contains 151 cycles. From Table 1, it can be learned that 151 cycles are different from others, those cycles shown up for once in 2018. In this case, we would ignore those cycles. In general, we would focus on the types which contain most cycles. For example, the type 2 contains 49 most similar cycles, type 8 contains 43 most similar cycles. In this case, we selected 1 cycle from type 2 and 1 cycle from type 8.

Table 2. The summary of the groups condition of the individual cycles

Folder_Name	Num_Files
Type Unique	151
Type 2	49
Type 8	43
Type 6	20
Type 3	19
Type 1	18
Type 13	11
Type 15	10
Type 4	10
Type 9	10

Figure 14 shows the examples of 2 cycles from type 2 and type 8, receptivity. The powers of both of those cycles are from -1 to 1. The negative power value represents the battery discharge processing, and the positive power value represents the battery charge processing. The blue box represents the time of charge/discharge, and the yellow line represent the rest time of the battery. The hours of charge are similar; however, the hours of discharge are different. Then those two kinds of cycles are grouped into different group. The battery scientist can cross check the plots and make the final decision that combine them or not. The application allowed battery scientist to choose and save the cycles by themselves.

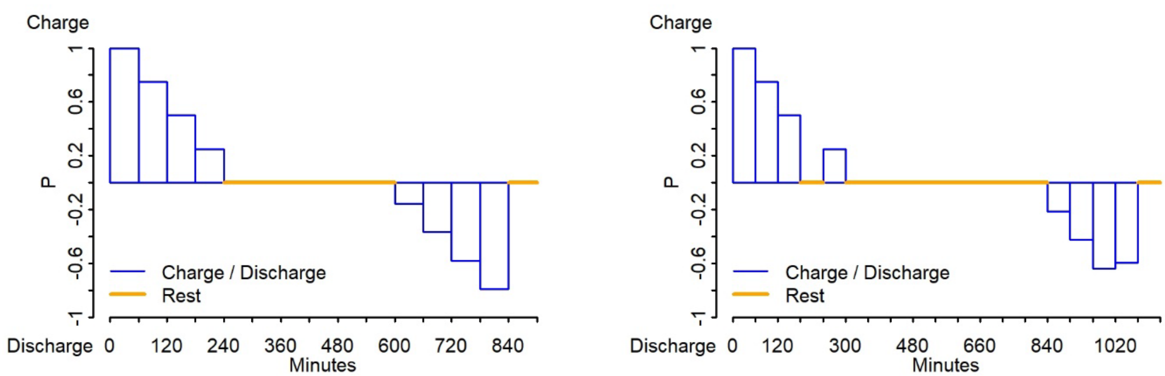

a) Cycle 4 b) Cycle 60

Figure 14. Time series plots of individual cycles. a) Cycle 4 was from the type 2 and b) Cycle 60 was from type 8

Figure 15 shows the different cycles from the different types. In Fig 9, the most similar cycle from the same type is shown. For example, the cycle 48 has the same pattern with the cycle 4 which were from type 2. Cycle 48 took longer time to rest when the percentage of the SOC was 50%. To make those 2 cycles which are grouped together, we ignore the rest time. Then, the more cycles are grouped into the same group.

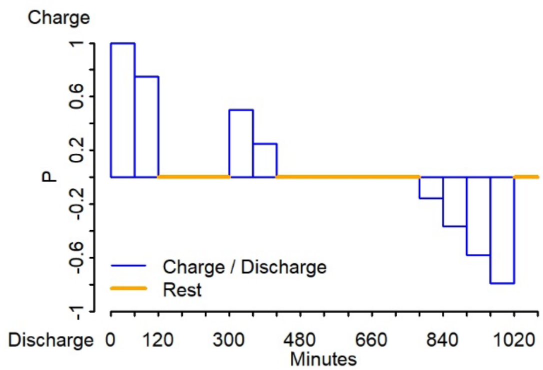

Figure 15. The time series plot of cycle 48

The simplify cycles can help the battery scientists to choose the proper number of cycles to test the battery and provide the solid recommend cycle into the real work.

Linking this part to battery designer enables to break down the cycles of ESS to single cell cycles, test protocol for single cells.

2.2.2. Frequency regulation data analysis

Frequency Regulation (or just “regulation”) always ensures the balance of electricity supply and demand, particularly over time frames from seconds to minutes. When supply exceeds demand the electric grid frequency increases and vice versa.

In this work, we choose MISO (Midcontinent Independent System Operator) with 1MW and 4 MWh frequency regulation data in 2018 to get the single cycles.

The actual battery power of this data set is from -1 MW to 1 MW. The battery SOC is from 0 to 100%. Figure 16 is the time series plot of the regulation data of MISO. The red line represents the battery charge and discharge power, and the blue line represents the SOC percentage. From Fig.1, it can be learned that the individual cycles of the SOC are different. The resolution of the time series data is 15 minutes.
To study the similarity of those cycles, we choose the cluster method.

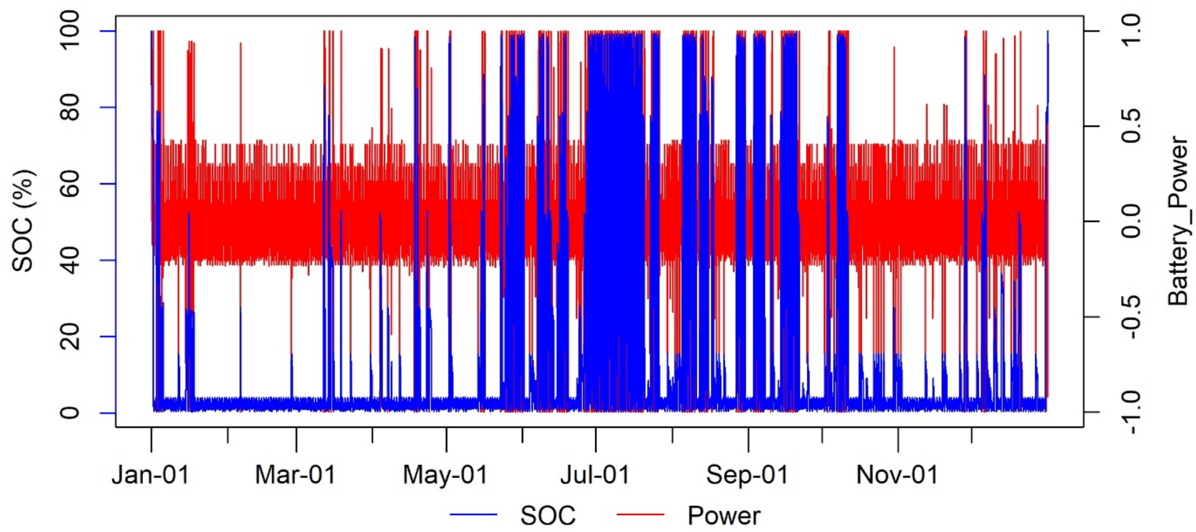

Figure 16. Time series plot of MISO regulation data with 1MW and 4 MWh

In this work, we choose the 90% SOC as the threshold to get the individual cycles. Then we get 65 cycles of the 2018 of MISO.

If we took the 90% as the threshold to get a whole single cycle, then during the cool season, less cycles are obtained, and during the hot season, more cycles are obtained. For example, we choose 2 cycles to show the result.

Figure 17. A is the first cycle of the regulation data, the whole cycle was from the beginning of the 2018 to middle of the April. The total hour of this time was 2574 hours. Most of the time, the battery was taking rest and it didn't fully charge or discharge. Figure 17. B shows a cycle during the summer, it was from 1:30 PM of the June 30 to 7:30 AM to July 1st. The total hour of the whole cycle was 18 hours. To simplify the pattern of the charge and discharge, during the cool season, we choose the fully discharged (the left blue line) and fully charged (the right blue line) data as a whole cycle, then the data between them were ignored.

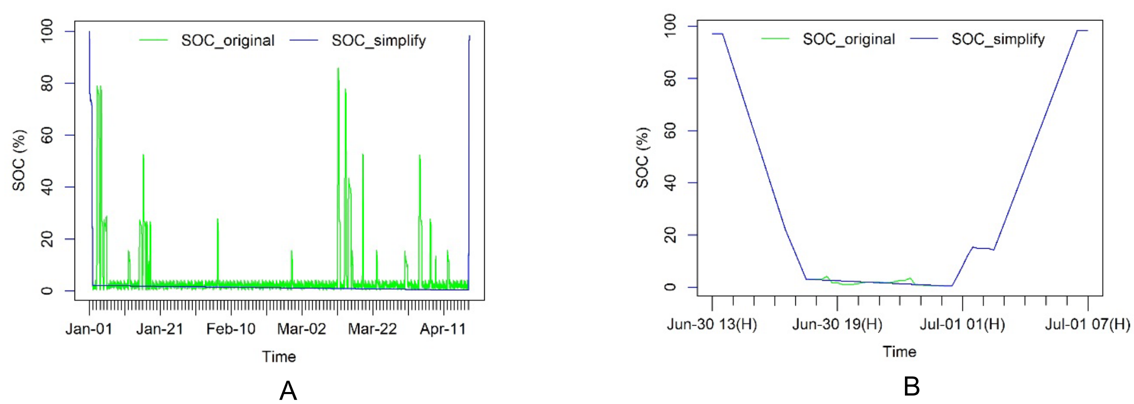

Figure 17. Time series plots of different cycles

Statistical analysis

Dynamic time wrapping

Even the cycle was simplified, the lengths of cycles are different. To study the similarity of the cycles, we applied the dynamic time wrapping to compute the distance between any two cycles.

The DTW method calculates an optimal match between two given sequences by using certain restriction and rules. For any two of the sequency, for sequency i which is from 1 to n, and sequency j which is from 1 to m. The DTW should be qualify the continuity condition. In this work, we removed the points which were not on the fully charge/discharge side and considered them as a continuous time series.
To calculate the distance, the first index of two sequencies should be matched, and the last index of two sequencies should be matched. The mapping of the indices from the first sequency to indices from the other sequency should be monotonically increasing. Then we can get the matrix of any two cycles. Based on the matrix, we applied the K-means clustering and Hierarchical clustering to cross check the similarity of those cycles.
Clustering is a most popular unsupervised machine learning and commonly used technique for classification. In this work, K-means clustering, and Hierarchical clustering were chosen.
K-means clustering
K-means clustering is used to classify data based on the different clustering distance such as Euclidean distance, Manhattan distance, Pearson correlation distance and other types of distance. The goal of the K-means clustering is to partition a given dataset into a set of k groups, where k represents the number of the pre-specified number of clusters.
Elbow method
To get the optimal clusters, we use the Elbow method to help determine the number of K. The minimum total within-cluster variation or total within-cluster sum of square should be minimized:

$$minimize(\sum_{k=1}^{k} W(C_k))$$

where C_k is the K^{th} cluster and the $W(C_k)$ is the within-cluster variation. The total within-cluster sum of square (wss) measures the compactness of the clustering. In this work, we assigned 2 to 8 to get the clusters.

1) Computer the clustering result by using different k (from 2 to 8).
2) For each k, the total within-cluster sum of square (wss) was obtained.
3) The optimized k can be obtained by comparing the wss.

Silhouette method
The silhouette method computes silhouette coefficients of each point that measure how much a point is similar to its own cluster compared to other clusters. To find the silhouette coefficient of a given point m:

1) Compute the average distance of point m with all other points in the same clusters A as A(m).
2) Compute the average distance of point m with all the points in the closest cluster to cluster A as B(m)
3) The silhouette coefficient can be obtained.

$$s(m) = \frac{B(m) - A(m)}{max(B(m), A(m))}$$

From the s(m) score, we can get the point(s) with negative score(s). Those points may have the different characters with other points of the same cluster.
In this work, we applied the silhouette distance to find the cycle which with lower score of the silhouette distance.
Hierarchical clustering
Hierarchical clustering is an alternative approach to K-means clustering for identifying groups for a given dataset. Hierarchical clustering starts by treating each observation as a single cluster, then a set of nested clusters are arranged. To get a tree shaped cluster, the following steps are needed.

1). If the distance of two clusters is close, then they will be put together.
2) The most similar clusters will be merged together.

The output of the Hierarchical cluster is a dendrogram, it is easy to visualize.

Results

As we mentioned, the value of K is from 2 to 8. Then use the elbow method to choose an optimized number of K. For this dataset, the recommend number of k is 3. 3 clusters were obtained from the K-means cluster in Figure 18 (a). Cluster 1 and cluster 3 contain more cycles and the cycles of cluster 2 are centralized.

The silhouette method can be as a backup to find the different cycle(s) from a specific cluster in Figure 18 (b). A cycle's silhouette distance is less than 0, so this cycle was picked up and marked as a special one.

a) K-means cluster

b) Silhouette distance

Figure 18. The results of the K-means clustering

To study the cluster results well, we cross check the result of Hierarchical clustering. For the Hierarchical clustering, 5 groups are emphasized. The first 3 clusters can be grouped together as a cluster. The cycles which are far from the center one would have the different pattern with the center one. Most of the cycles are grouped into the fourth clusters that means most of those cycles are similar with others.

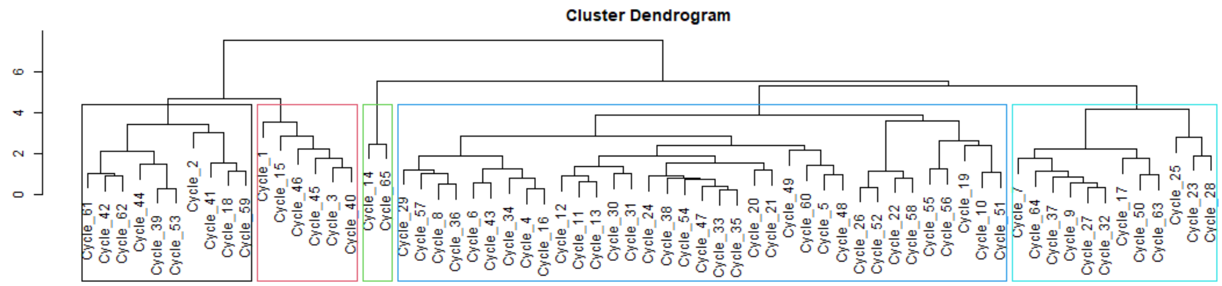

Figure 19. The result of Hierarchical clustering

Both the k-means and hierarchical clustering provided the recommend clusters and the cycles which are different from others within a cluster.
The goal of the analysis is to find the most similar and special cycles. By studying the results of the k-means and Hierarchical clustering, we selected 8 cycles with most of the different patterns. Those cycles can help to determine which cycle should be used for the testing of the designed batteries and check the performance of different cycles.

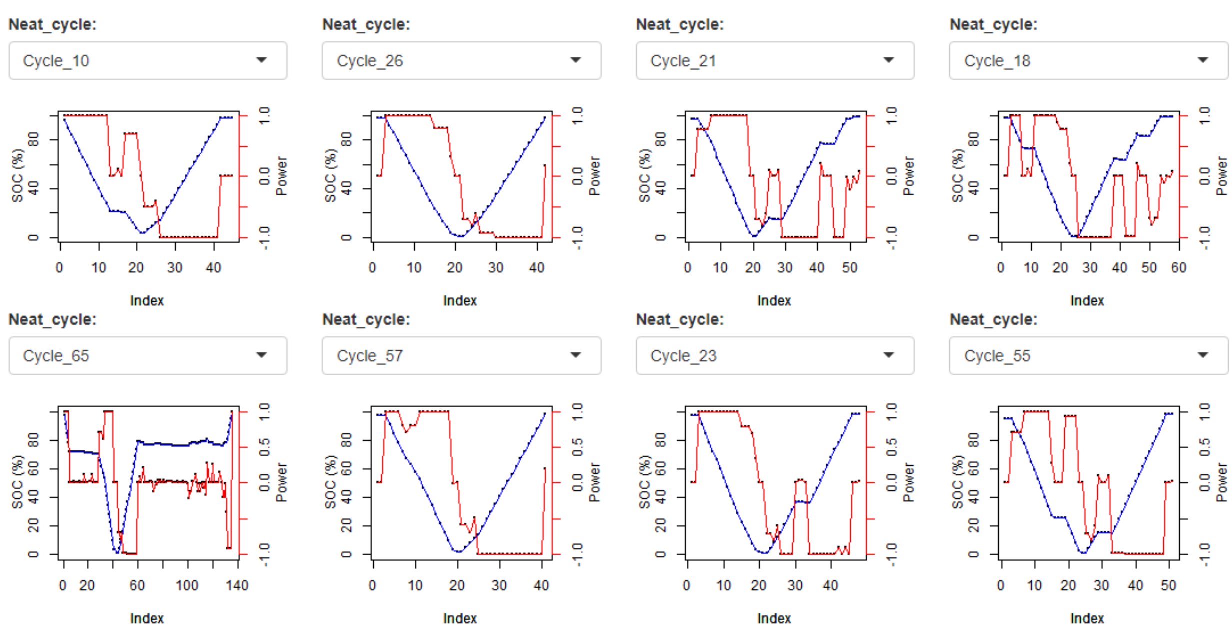

Figure 20. The time series plot of selected neat cycles by using k-means and Hierarchical clustering analysis

By studying the performance cycles, the battery design scientists can recommend the optimized cycles to charge or discharge during operating.

Linking this part to battery designer enables to break down the cycles of ESS to single cell cycles, test protocol for single cells.

2.2.3. Software development

With the data analysis on grid-scale energy storage in section 2.2.2, the final software is achieved. Figure 21 shows the interface of the ESS data analysis, including arbitrage energy data analysis (Figure 21a) and frequency regulation data analysis (Figure 21b and 21c).

(a)

(b)

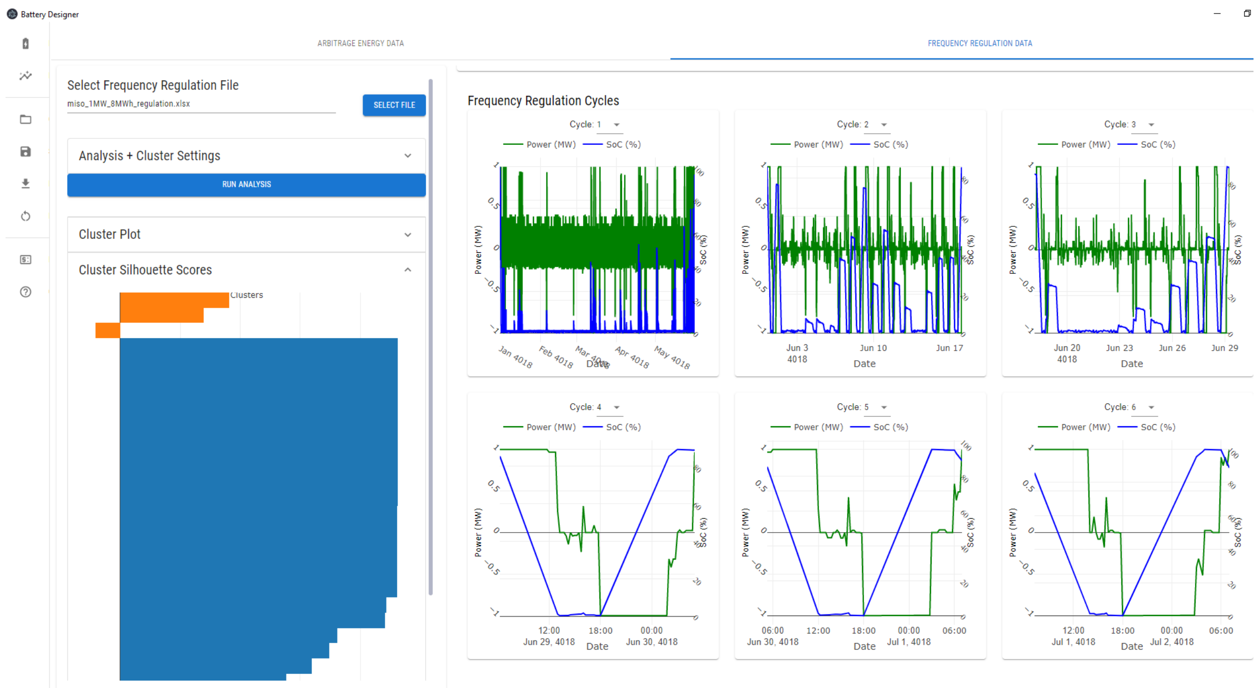

(c)

Figure 21. The interface of grid-scale energy storage system data analysis software, (a) arbitrage energy data analysis; (b)(c) frequency regulation data analysis.

2.3 Graphite/LFP pouch cell fabrication and testing

To demonstrate the superiority of the software in practical application, we fabricated some graphite/LFP pouch cells with different design and testing to get data for verification.

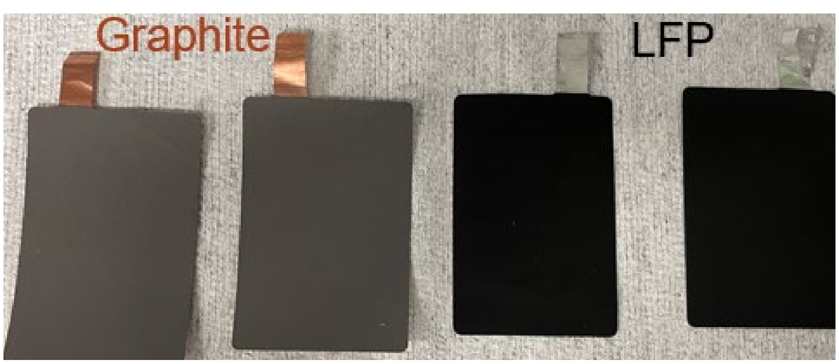

(A) (B)

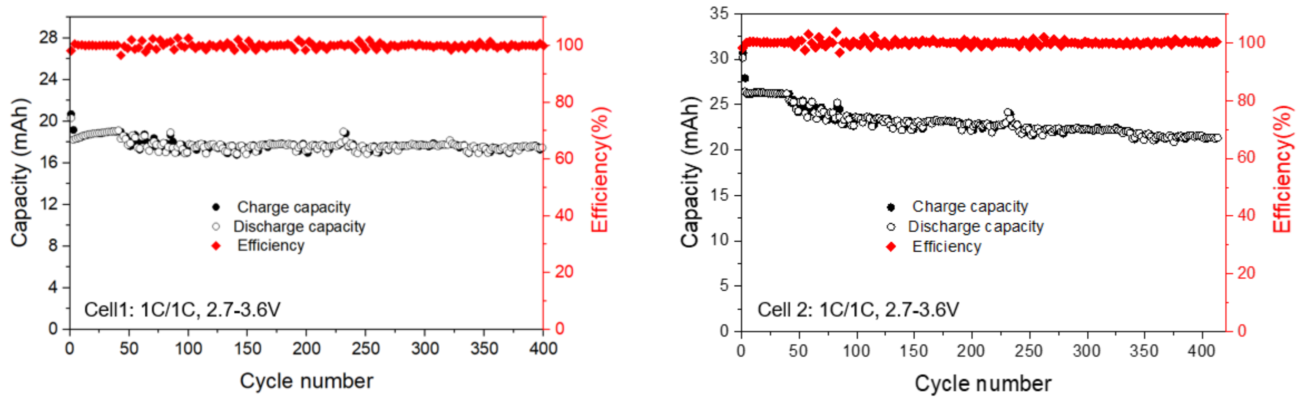

(C)

Figure 22. LFP/Gr. Pouch cell with different design. (A) Graphite anodes and LFP cathodes; (B) LFP/Gr. Pouch cells; (C) Cycling performance of two of the batteries. Cell size: 40*70mm

We have assembled the first batch cells to verify the design software and fabrication process, the designs of cells provided by design software. Figure 22A shows graphite anodes and LFP cathodes which we coated. Figure22B shows the fresh single layer pouch cell before test which we assembled with graphite anode and LFP cathode. Figure 22C indicate that the cycling performance of pouch cells which output by design software and as-build manufacturing line are very good for verification. 0.5 Ah and 1 Ah pouch cells are also produced.

Using the software choose two designs (Figure 23 (A) and (B)) to fabricate some cells and test with corresponding single cell testing arbitrage and frequency regulation protocols which provided by software. We choose MISO with 1MW and 2MWh arbitrage energy data (Figure 24) and frequency regulation data (Figure 26) in 2018 to get the single cycle and break down to single cell test protocol (table 3 and table 4).

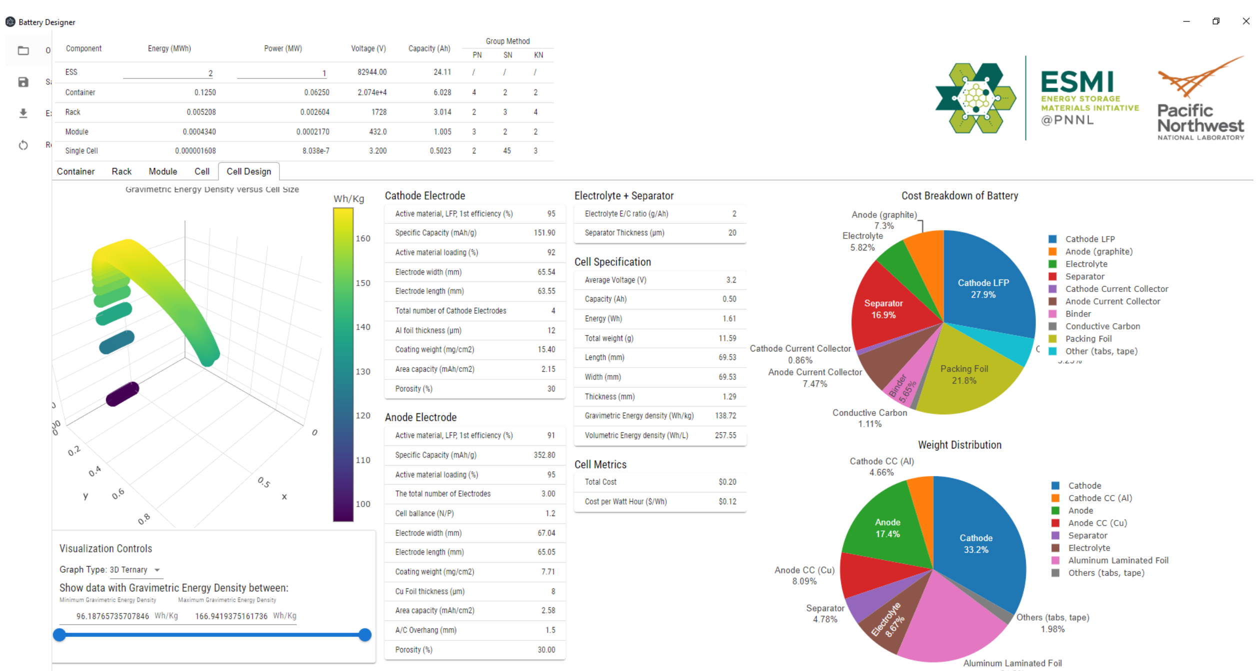

(A)

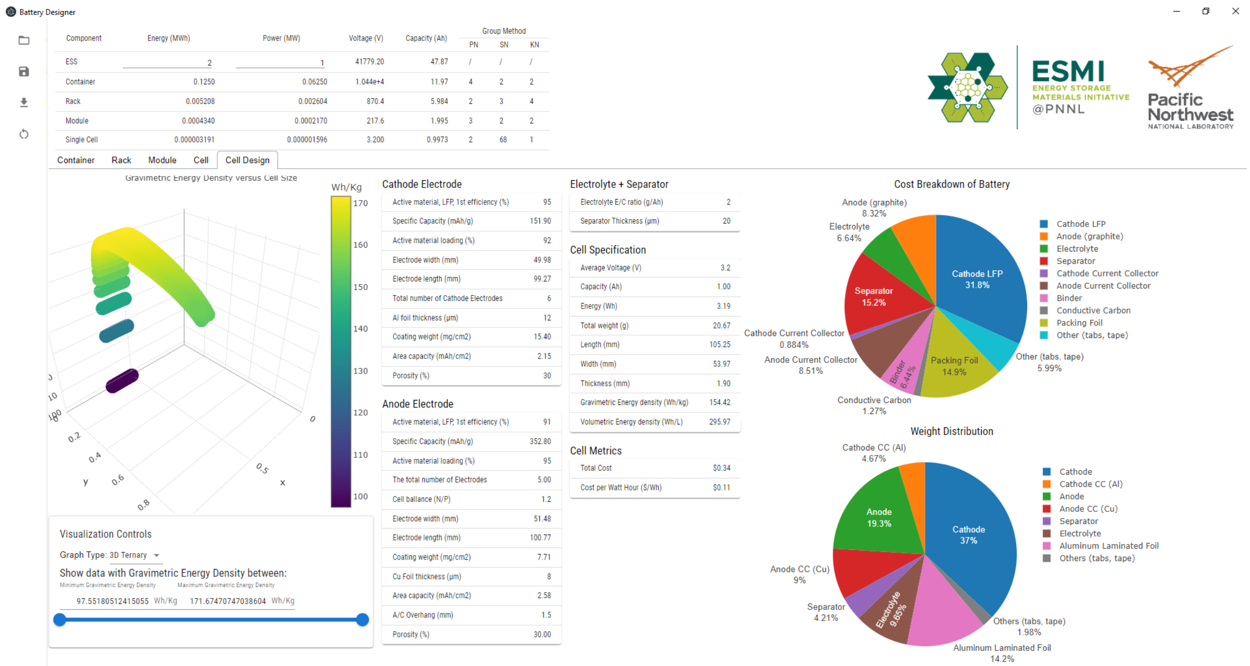

(B)

Figure 23. 0.5Ah and 1 Ah LFP/Gr. Pouch cell design. (A) 0.5Ah LFP/Gr. pouch cell design parameters; (B) 1 Ah LFP/Gr. Pouch cell design parameters.

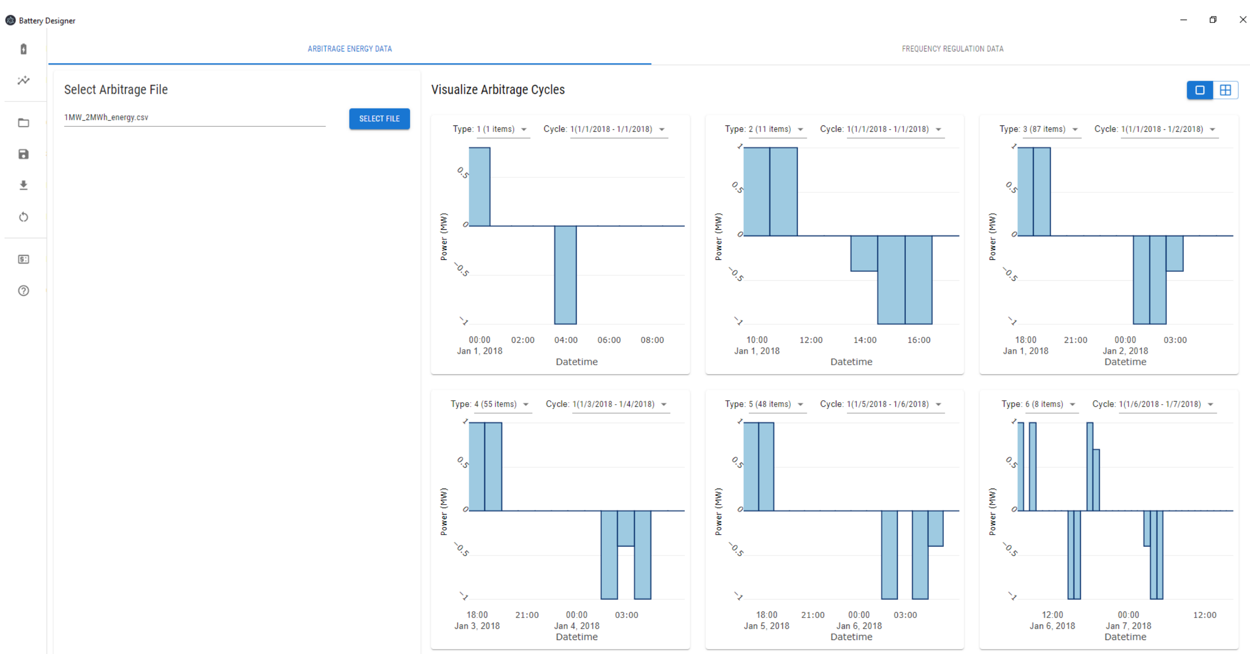

Figure 24. MISO with 1MW and 2MWh arbitrage energy data in 2018 analysis

Table 3. Single cell arbitrage test protocols for two designs

1 Ah single cell
1. 1.28W discharge 1h
2. rest 3h
3.1.6W charge 1h
4.rest 5h
5.1.6W discharge 2h
6. rest 2h
7.0.64W charge 1h
8.1.6 W charge 2h
9. rest 1h
10. 1.6W discharge 2h
11. rest 5h
12. 1.6W charge 2h
13. 0.64W charge 1h
14. rest 3h
15. 1.6W discharge 2h
16. rest 5h
17.0.64W charge1h
18. 1.6W charge 2h
19.rest 1h
20.1.6W discharge 2h
21. rest 5h
22.0.64W charge1h
23. 1.6W charge 2h
24. rest 3h
25. 1.6W discharge 2h
26. rest 5h
27. 1.6W charge 2h
28.0.64W charge1h
29.rest 1h
30. 1.6W discharge 2h
31. rest 5h
32.1.6 W charge 1h
33.0.64W charge 1h
34. 1.6 W charge 1h
35.rest 2h
36. 1.6 W discharge2h
37.rest 5h
38. 1.6 W charge 2h

0.5 Ah single cell
1. 0.64W discharge 1h
2. rest 3h
3.0.8W charge 1h
4.rest 5h
5.0.8W discharge 2h
6. rest 2h
7.0.32W charge 1h
8. 0.8 W charge 2h
9. rest 1h
10. 0.8W discharge 2h
11. rest 5h
12. 0.8W charge 2h
13. 0.32W charge 1h
14. rest 3h
15. 0.8W discharge 2h
16. rest 5h
17.0.32W charge1h
18. 0.8W charge 2h
19.rest 1h
20.0.8W discharge 2h
21. rest 5h
22.0.32W charge1h
23. 0.8W charge 2h
24. rest 3h
25. 0.8W discharge 2h
26. rest 5h
27. 0.8W charge 2h
28.0.32W charge1h
29.rest 1h
30. 0.8 W discharge 2h
31. rest 5h
32.0.8 W charge 1h
33.0.32W charge 1h
34. 0.8 w charge 1h
35.rest 2h
36. 0.8W discharge2h
37.rest 5h
38. 0.8 W charge 2h

39. 0.64W charge 1h	39. 0.32W charge 1h
40. rest 1h	40. rest 1h
41. 1.6W discharge 2h	41. 0.8W discharge 2h
42 rest 6h	42 rest 6h
43. 1.6w charge 1h	43. 0.8w charge 1h
44. 0.64 W charge 1h	44. 0.32 W charge 1h
45.1.6W charge 1h	45.0.8W charge 1h
46. rest 2h	46. rest 2h
47. 1.6W discharge 2h	47. 0.8W discharge 2h
48. rest 5h	48. rest 5h
49.0.64w charge 1h	49.0.32w charge 1h
50.1.6W charge 2h	50. 0.8W charge 2h
51.1.6W discharge 2h	51. 0.8W discharge 2h
52. rest 7h	52. rest 7h
53. 1.6W charge 1h	53. 0.8W charge 1h
54 rest 1h	54 rest 1h
55. 1.6W charge 1h	55. 0.8W charge 1h
56. 0.64W charge 1h	56. 0.32W charge 1h
57. rest 1h	57. rest 1h
58. 1.6w discharge 1h	58. 0.8w discharge 1h
59. rest 1h	59. rest 1h
60. 1.6W discharge 1h	60. 0.8W discharge 1h
61. rest 5h	61. rest 5h
62. 1.6W charge 2h	62. 0.8W charge 2h
63.rest 1h	63.rest 1h
64. 1.6W discharge 1h	64. 0.8W discharge 1h
65.1.12W discharge 1h	65.0.56W discharge 1h
66.rest 7h	66.rest 7h
67. 0.64W charge 1h	67. 0.32W charge 1h
68.1.6W charge 2h	68.0.8W charge 2h
69. rest 11h	69. rest 11h
70. 1.6 W discharge 2h	70. 0.8 W discharge 2h
71.rest 6h	71.rest 6h
72. 0.64W charge 1h	72. 0.32W charge 1h
73. 1.6W charge 1h	73. 0.8W charge 1h
74. rest 1h	74. rest 1h
75. 1.6W charge 1h	75. 0.8W charge 1h
76. rest 13h	76. rest 13h
77. 1.6W discharge 2h	77. 0.8W discharge 2h
78.rest 6h	78.rest 6h
79.0.64W charge 1h	79.0.32W charge 1h

80. 1.6W charge 2h	80. 0.8W charge 2h
81. rest 2h	81. rest 2h
82. 1.6W discharge 2h	82. 0.8W discharge 2h
83.rest 5h	83.rest 5h
84.0.64 W charge 1h	84.0.32W charge 1h
85. 1.6w charge 2h	85. 0.8w charge 2h
86. rest 1h	86. rest 1h
87. 1.6W discharge 2h	87. 0.8W discharge 2h
88.rest 5h	88.rest 5h
89.1.6W charge 2h	89.0.8W charge 2h
90.rest 1h	90.rest 1h
91. 0.64W charge 1h	91. 0.32W charge 1h
92. rest 13h	92. rest 13h
93. 1.6w discharge 2h	93. 0.8w discharge 2h
94. rest 6h	94. rest 6h
95.0.64 W charge 1h	95.0.32W charge 1h
96. 1.6w charge 2h	96. 0.8W charge 2h
97. rest 13h	97. rest 13h
98. 1.6w discharge 2h	98. 0.8W discharge 2h
99.rest 5h	99.rest 5h

0.5Ah and 1Ah pouch cells were produced (Figure 24a). Using the single cell test protocol to test the 0.5Ah and 1Ah pouch cells, as shown Figure 25. (a) Power and voltage curve of 0.5Ah and 1Ah pouch cell testing with arbitrage energy single cell test protocol; (b) arbitrage energy single cycles, the results show both designs run very well. The performance meets the charge and discharge power requirements.

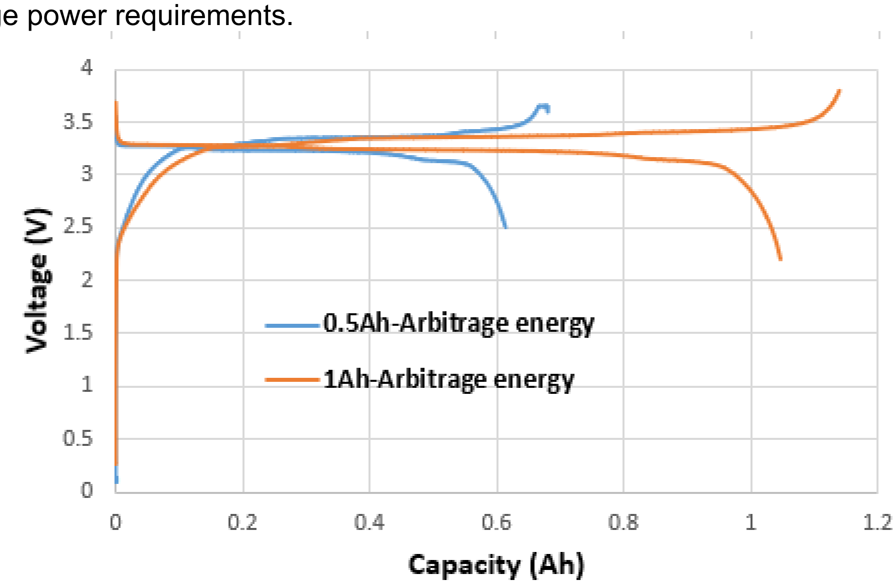

Figure 24a. Formation of 0.5Ah and 1Ah pouch cells.

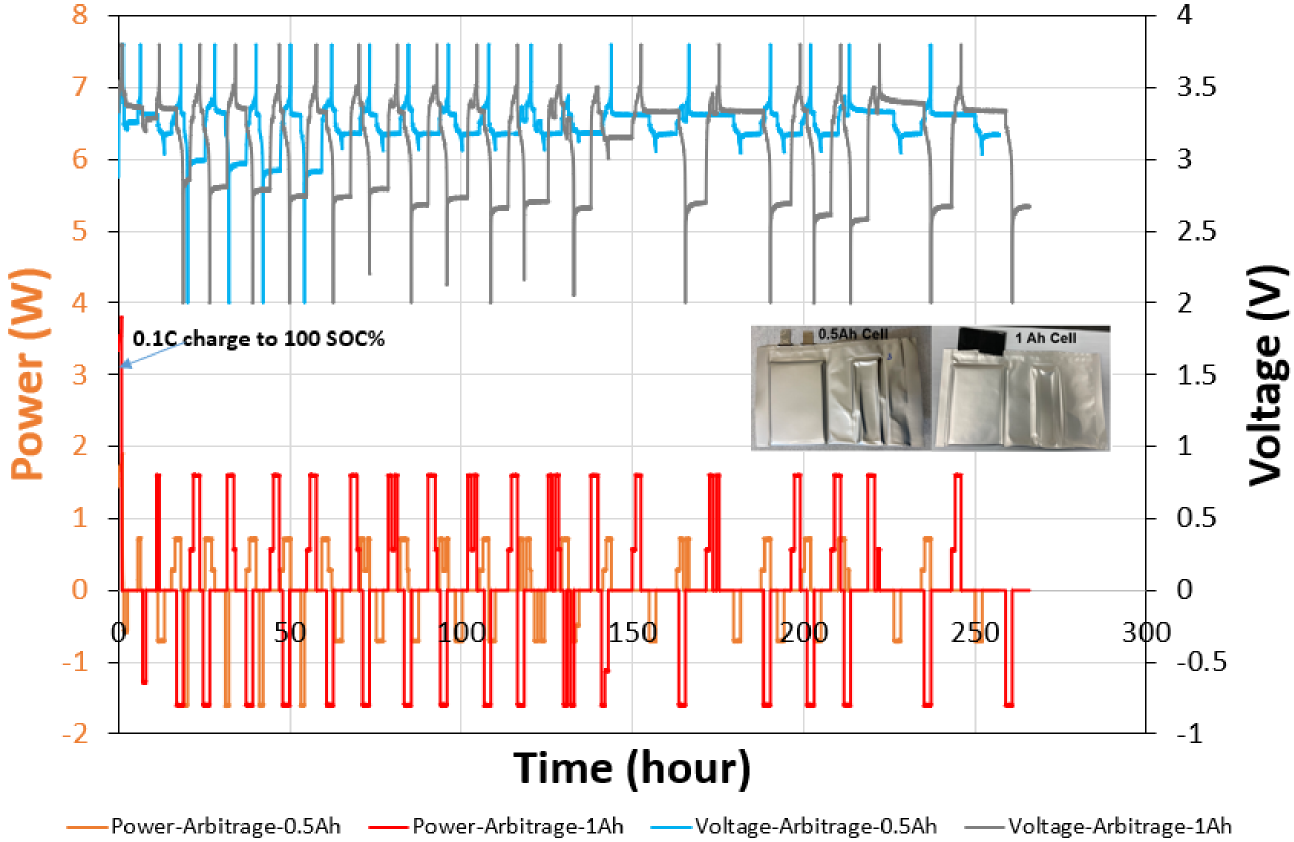
0.1C charge to 100 SOC%
0.5Ah Cell
1 Ah Cell
Power (W)
Voltage (V)
Time (hour)
Power-Arbitrage-0.5Ah
Power-Arbitrage-1Ah
Voltage-Arbitrage-0.5Ah
Voltage-Arbitrage-1Ah

(a)

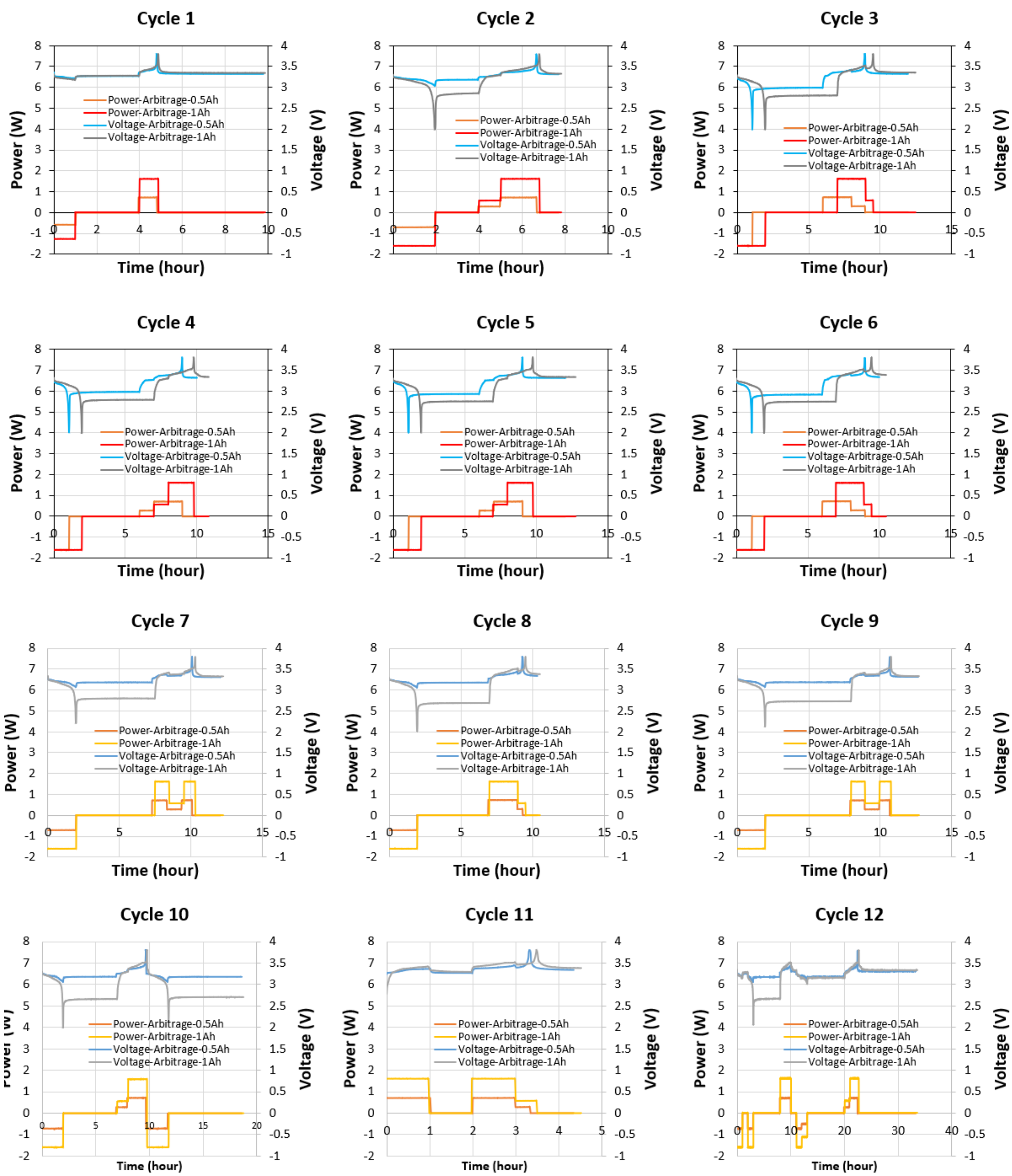
Cycle 1
Cycle 2
Cycle 3
Cycle 4
Cycle 5
Cycle 6
Cycle 7
Cycle 8
Cycle 9
Cycle 10
Cycle 11
Cycle 12
Power-Arbitrage-0.5Ah
Power-Arbitrage-1Ah
Voltage-Arbitrage-0.5Ah
Voltage-Arbitrage-1Ah
Power (W)
Voltage (V)
Time (hour)

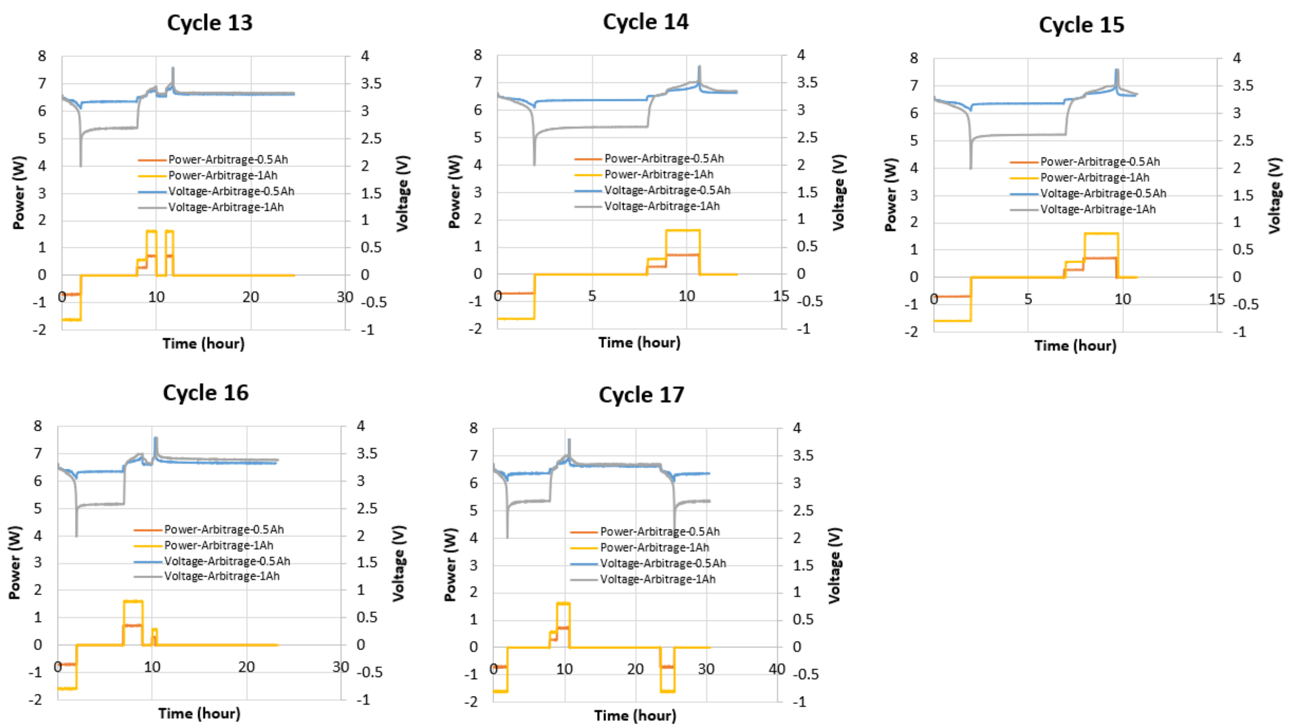

(b)

Figure 25. (a) Power and voltage curve of 0.5Ah and 1Ah pouch cell testing with arbitrage energy single cell test protocol; (b) arbitrage energy single cycles.

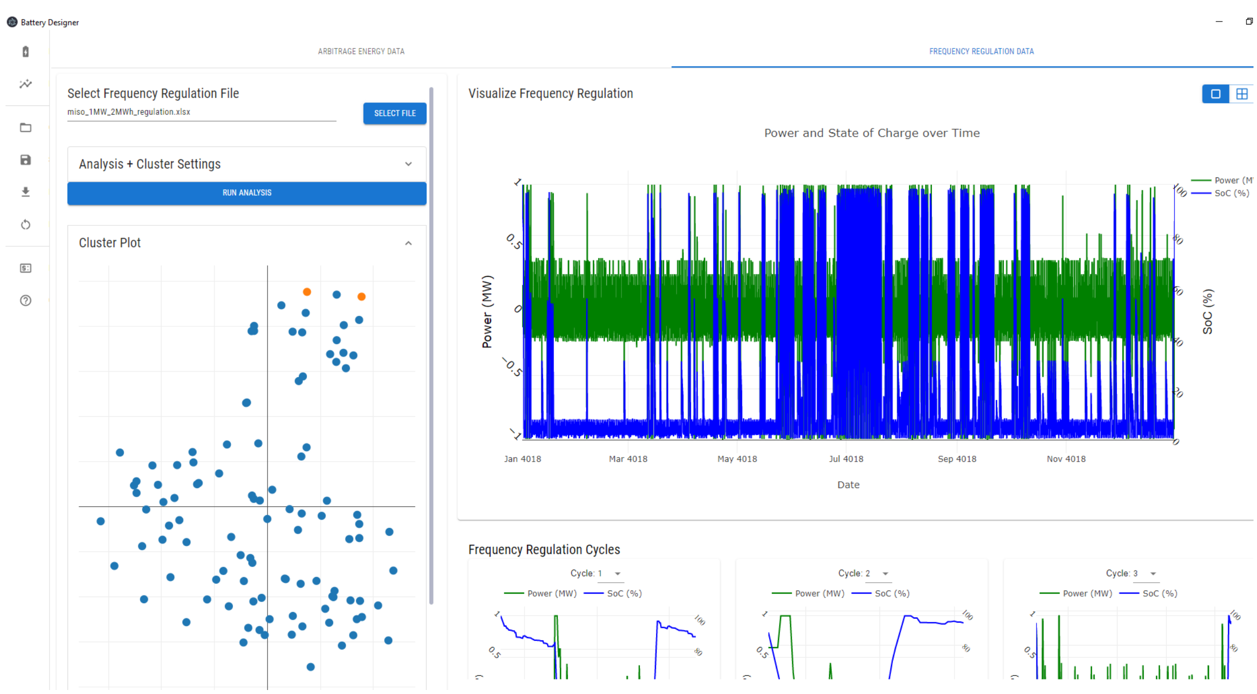

Figure 26. MISO with 1MW and 2MWh frequency regulation data in 2018 analysis

Table 4. Single cell frequency regulation test protocols for two designs

1Ah Cell	0.5Ah Cell
1. 0.16 W discharge 5h	1. 0.08 W discharge 5h
2. rest 2h	2. rest 2h
3.0.16W discharge 1h	3.0.08W discharge 1h
4.rest 1h	4.rest 1h
5.0.07W discharge 2h	5.0.035W discharge 2h
6 rest 2h	6 rest 2h
7.0.03W discharge 1h	7.0.015W discharge 1h
8 rest 1h	8 rest 1h
9.0.03W discharge 1h	9.0.015W discharge 1h
10. rest 2h	10. rest 2h
11. 0.13 W discharge 1h	11. 0.065W discharge 1h
12. rest 1h	12. rest 1h
13. 0.34W discharge 1h	13. 0.17W discharge 1h
14 rest 1h	14 rest 1h
15. 0.02W discharge 1h	15. 0.01W discharge 1h
16 rest 3h	16 rest 3h
17.0.04W discharge 2h	17.0.02W discharge 2h
18.rest 1h	18.rest 1h
19.0.19W charge 1h	19.0.095W charge 1h
20.rest 1h	20.rest 1h
21. 0.03W charge 1h	21. 0.015W charge 1h
22.0.06W discharge1h	22.0.03W discharge1h
23. rest 1h	23. rest 1h
24. 0.06W discharge1h	24. 0.03W discharge1h
25. rest 2h	25. rest 2h
26. 0.04W discharge 1h	26. 0.02W discharge 1h
27.rest 2h	27.rest 2h
28.0.04W discharge 4h	28.0.02W discharge 4h
29.rest 3h	29.rest 3h
30 0.03W discharge 1h	30 0.015W discharge 1h
31. rest 3h	31. rest 3h
32. 0.03W discharge 1h	32. 0.015W discharge 1h
33. rest 3h	33. rest 3h
34. 0.17W discharge 1h	34. 0.085W discharge 1h
35. rest 1h	35. rest 1h
36. 0.01W discharge 2h	36. 0.005W discharge 2h

37. 0.02W discharge 2h
38. 0.18W discharge 1h
39. rest 6h
40.0.12W charge 1h
41. rest 1h
42. 0.28W charge 1h
43.1.6W discharge 4h
44. 1.12 discharge 1h
45. 0.8W discharge 1h
46. 0.96 discharge 2h
47. rest 2h
48. 0.11W discharge 1h
49. rest 1h
50. 0.12 charge 2h
51. rest 1h
52. 0.28W charge 1h
53.0.68W discharge 1h
54. rest 1h
55.0.04W discharge 2h
56. rest 1h
57. 0.01W discharge 1h
58. rest 2h
59. 0.13W charge 3h
60. rest 1h
61.0.14W discharge 1h
62. rest 2h
63. 0.14 discharge 1h
64.0.2W charge 1h
65. 0.04W charge 3h
66.rest 6h
67.0.08W discharge 1h
68. rest 1h
69.0.11W discharge 1h
70. rest 3h
71. 0.12W charge 2h
73.rest 3h
74.0.2W charge 1h
75.rest 1h
76. 0.04W charge 1h

37. 0.01W discharge 2h
38. 0.09W discharge 1h
39. rest 6h
40.0.06W charge 1h
41. rest 1h
42. 0.14W charge 1h
43.0.8W discharge 4h
44. 0.56 discharge 1h
45. 0.4W discharge 1h
46. 0.48 discharge 2h
47. rest 2h
48. 0.055W discharge 1h
49. rest 1h
50. 0.06 charge 2h
51. rest 1h
52. 0.14W charge 1h
53.0.34W discharge 1h
54. rest 1h
55.0.02W discharge 2h
56. rest 1h
57. 0.005W discharge 1h
58. rest 2h
59. 0.065W charge 3h
60. rest 1h
61.0.07W discharge 1h
62. rest 2h
63. 0.07 discharge 1h
64.0.1W charge 1h
65. 0.02W charge 3h
66.rest 6h
67.0.04W discharge 1h
68. rest 1h
69.0.055W discharge 1h
70. rest 3h
71. 0.06W charge 2h
73.rest 3h
74.0.1W charge 1h
75.rest 1h
76. 0.02W charge 1h

77. 0.06W discharge 1h
78. rest 1h
79.0.06W discharge 1h
80.rest 2h
81.0.15W discharge 1h
82.rest 2h
83. 0.04W discharge 4h
84.rest 1h
85.0.06W charge 1h
86. rest 1h
87.0.06W charge 1h
88.0.04W discharge 1h
89.rest 3h
90.0.03W discharge 1h
91.rest 3h
92.0.18W charge 2h
93. 0.02W charge 1h
94. 0.18W charge 1h
95. 0.04Wcharge 1h
96. rest 1h
97. 0.04W charge 1h
98. rest 1h
99.0.01W charge 3h
100. 0.33W charge 1h
101. 0.45W discharge 1h
102. rest 3h
103. 0.06W charge 1h
104. 0.22W charge 1h
105. rest 1h
106.0.37W charge 1h
107. 0.65W discharge 1h
108.rest 1h
109.0.17W discharge 1h
110.0.01W discharge 1h
111.rest 1h
112. 0.01W discharge 1h
113. rest 2h
114.1.11W charge 2h
115.1.27W charge 1h

77. 0.03W discharge 1h
78. rest 1h
79.0.03W discharge 1h
80.rest 2h
81.0.075W discharge 1h
82.rest 2h
83. 0.02W discharge 4h
84.rest 1h
85.0.03W charge 1h
86. rest 1h
87.0.03W charge 1h
88.0.02W discharge 1h
89.rest 3h
90.0.015W discharge 1h
91.rest 3h
92.0.09W charge 2h
93. 0.01W charge 1h
94. 0.09W charge 1h
95. 0.02Wcharge 1h
96. rest 1h
97. 0.02W charge 1h
98. rest 1h
99.0.005W charge 3h
100. 0.165W charge 1h
101. 0.225W discharge 1h
102. rest 3h
103. 0.03W charge 1h
104. 0.11W charge 1h
105. rest 1h
106.0.135W charge 1h
107. 0.325W discharge 1h
108.rest 1h
109.0.085W discharge 1h
110.0.005W discharge 1h
111.rest 1h
112. 0.005W discharge 1h
113. rest 2h
114.0.555W charge 2h
115.0.635W charge 1h

116. 1.11W charge 1h
117.0.16W discharge 1h
118.rest 2h

116. 0.555W charge 1h
117.0.08W discharge 1h
118.rest 2h

Another 0.5 Ah and 1Ah pouch cells were produced (Figure 26a). Using the single cell frequency regulation test protocol to test the 0.5Ah and 1Ah pouch cells, as shown Figure 27. (a) Power and voltage curve of 0.5Ah pouch cell testing with frequency regulation single cell test protocol; ((b) testing curve for 10-40 hours; (c) testing curve for 140-170 hours, and Figure 28. (a) Power and voltage curve of 1 Ah pouch cell testing with frequency regulation single cell test protocol; (b) testing curve for 20-50 hours; (c) testing curve for 220-250 hours, the results show both designs run very well. The performance meets the charge and discharge power requirements.

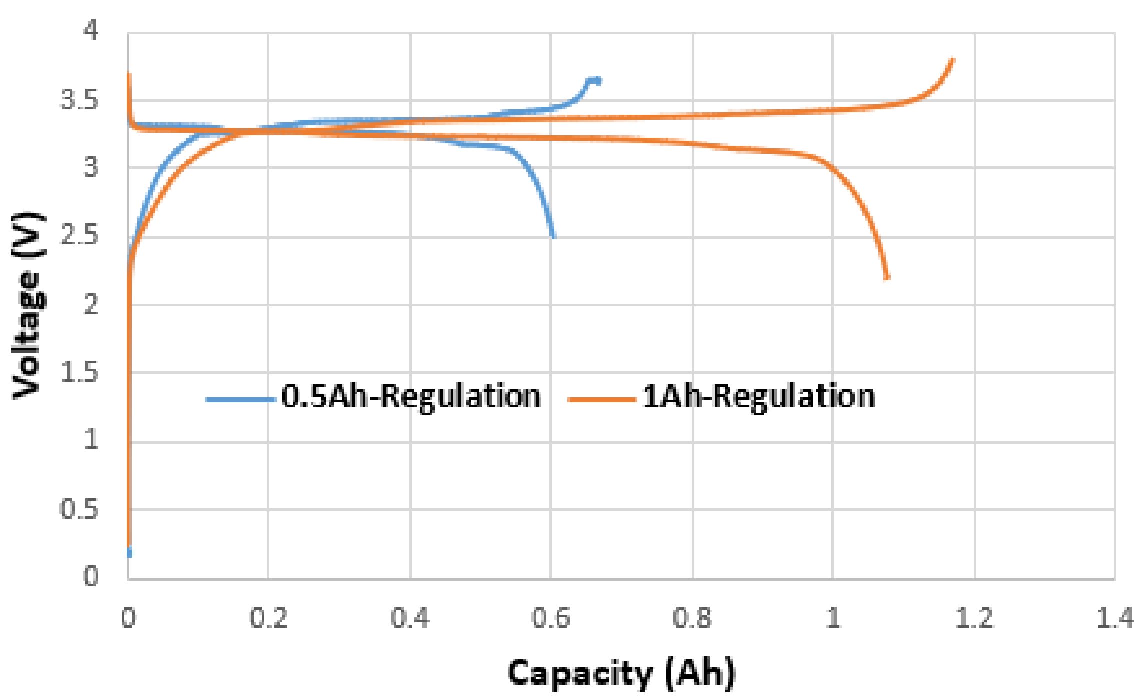

Figure 26a. Formation of another 0.5Ah and 1Ah pouch cells.

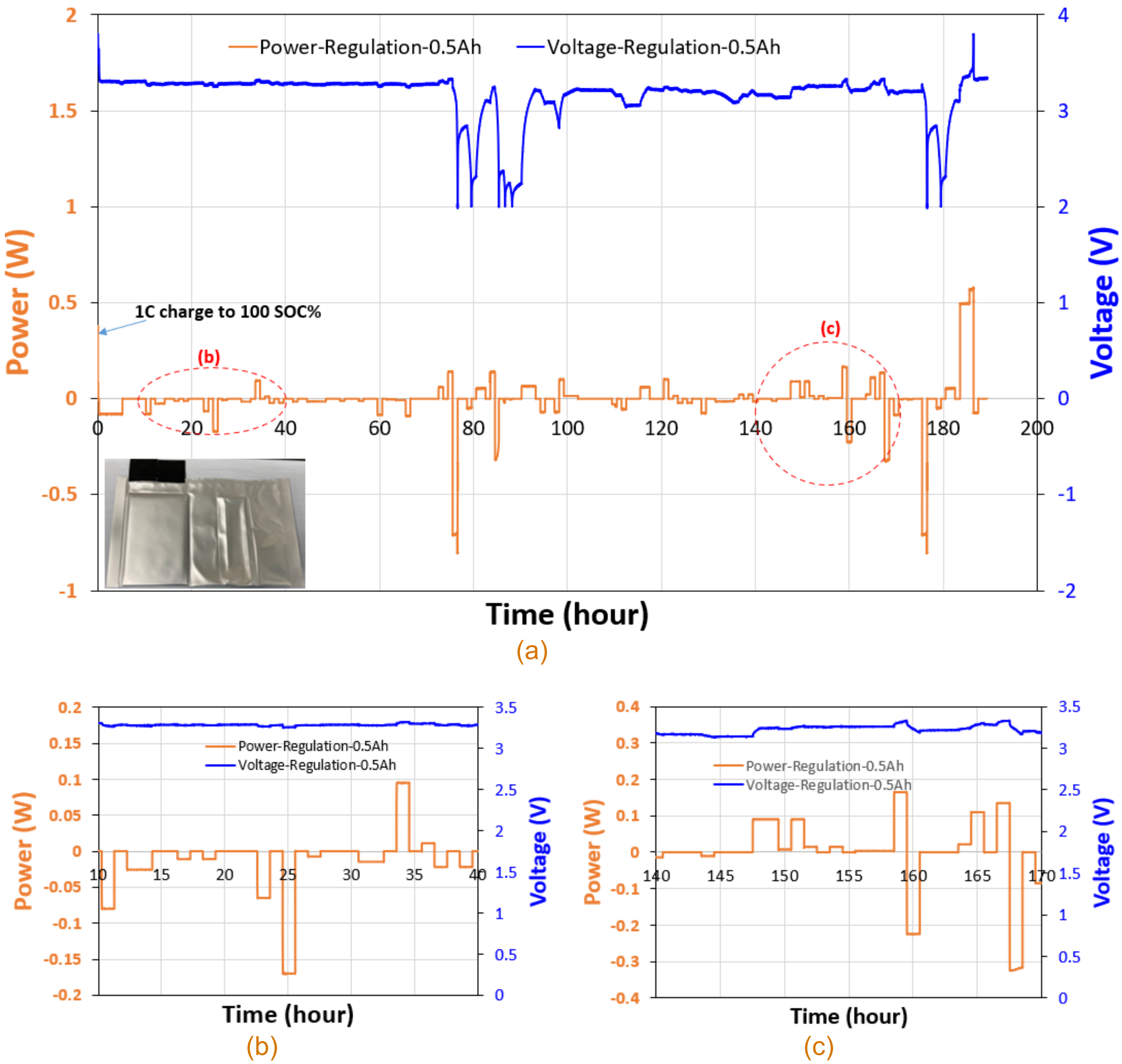

Figure 27. (a) Power and voltage curve of 0.5Ah pouch cell testing with frequency regulation single cell test protocol; (b) testing curve for 10-40 hours; (c) testing curve for 140-170 hours

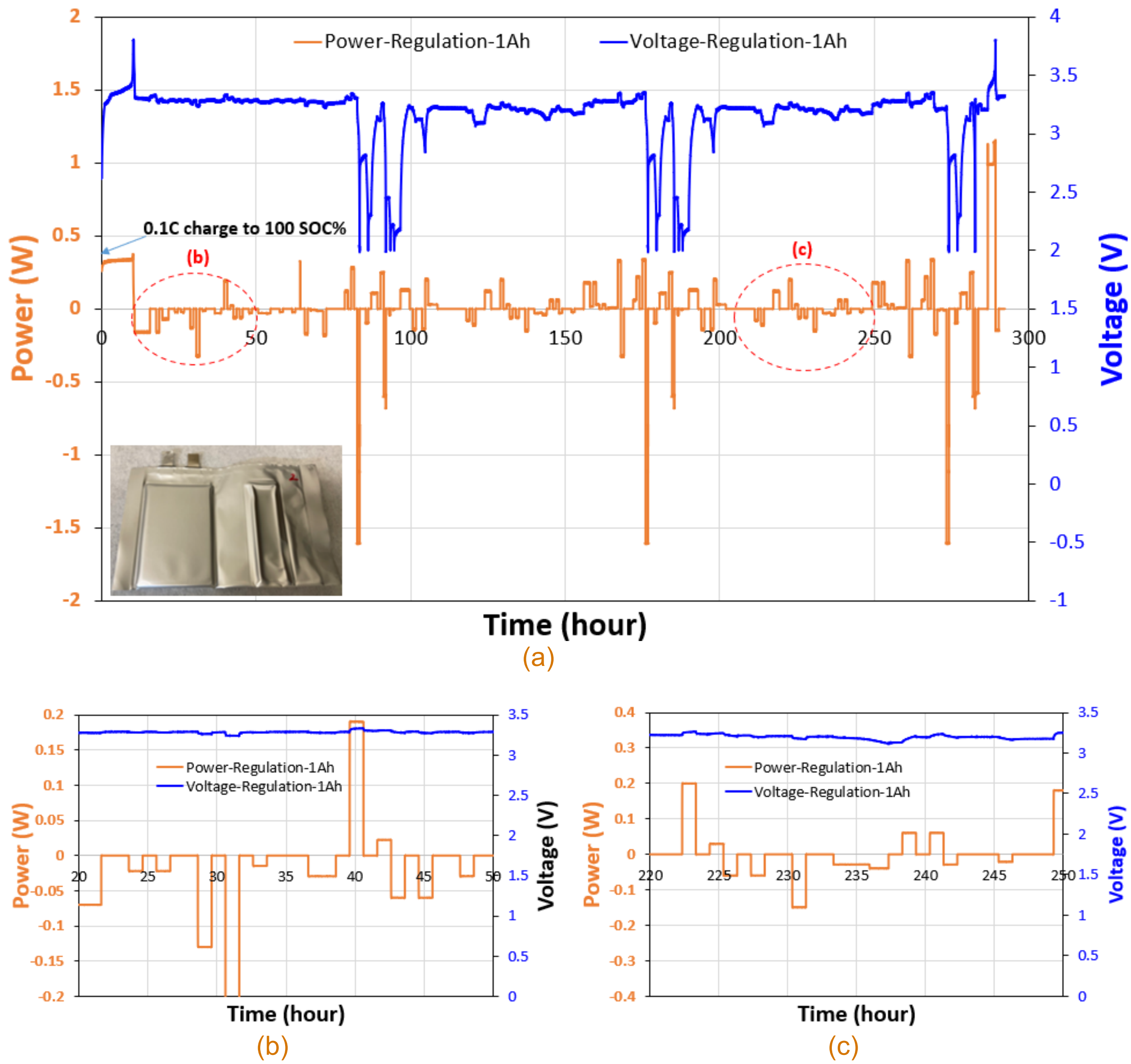

Figure 28. (a) Power and voltage curve of 1 Ah pouch cell testing with frequency regulation single cell test protocol; (b) testing curve for 20-50 hours; (c) testing curve for 220-250 hours

The cell testing was running very well with test protocols which provided by software, these result show the software can quickly sort/display charge and discharge levels of the battery throughout the year from different regions, and provide ESS breakdown to a single cell with the input requirements.

2.4 Summary

A software is developed to deliver optimal cell design parameters, material cost of cell, group method, ESS system breakdown and perform grid-scale energy storage system data analysis. Combined materials- and data-driven approaches, the software provides cost-competitive cell design for large-scale energy storage up to MWh scales for different regional requirements. Meanwhile, the APP can quickly analyze grid energy storage data from different regions and provide battery designs that match their performance and cost target.

1. The app was demonstrated as a toolkit for designing Graphite/LFP lithium-ion pouch cell for grid energy storage.

2. Visualize the analysis and decomposition of energy storage battery data in various regions.

3. The as-built Graphite/$LiFePO_4$ pouch cell manufacturing line and cell testing can be deployed to evaluate the cell design, as well as support other projects in electrolyte development, like safe electrolyte project in ESMI. This will enhance PNNL's role in graphite/LFP pouch cell manufacturing and testing in ESS application.

Contact PIs for software installation and use.

3.0 References

[1] C. J. Barnhart, and S. M. Benson, “On the importance of reducing the energetic and material demands of electrical energy storage,” *Energ Environ Sci,* vol. 6, no. 4, pp. 1083-1092, 2013.

[2] M. C. Kintner-Meyer, P. J. Balducci, W. G. Colella *et al.*, *National assessment of energy storage for grid balancing and arbitrage: Phase 1, WECC*, Pacific Northwest National Lab.(PNNL), Richland, WA (United States), 2012.

[3] D. Lindley, “Smart grids: The energy storage problem,” *Nature News,* vol. 463, no. 7277, pp. 18-20, 2010.

[4] C. Vartanian, and N. Bentley, "A123 systems' advanced battery energy storage for renewable integration." pp. 1-6.

[5] Jie Xiao, Yang Yang, Dianying Liu, and Zhiqun D Deng, Li-Batt Design App, Pacific Northwest National Laboratory, Richland, WA, USA

[6] J. Eyer and G. Corey, “Energy storage for the electricity grid: Benefits and market potential assessment guide,” Sandia National Laboratories, vol. 20, no. 10, p. 5, 2010.

[7] R. Sioshansi, P. Denholm, T. Jenkin, and J. Weiss, “Estimating the value of electricity storage in pjm: Arbitrage and some welfare effects,” Energy economics, vol. 31, no. 2, pp. 269–277, 2009.

Pacific Northwest National Laboratory

902 Battelle Boulevard
P.O. Box 999
Richland, WA 99354

1-888-375-PNNL (7665)

www.pnnl.gov